

# The influence of multiple stars on the high-mass stellar initial mass function and age-dating of young massive star clusters

C. Weidner<sup>1,2\*</sup>, P. Kroupa<sup>3†</sup> and T. Maschberger<sup>3,4‡</sup>

<sup>1</sup>*Departamento de Astronomía y Astrofísica, Pontificia Universidad Católica de Chile, Av. Vicuña MacKenna 4860, Macul, Santiago, Chile*

<sup>2</sup>*Scottish Universities Physics Alliance (SUPA), School of Physics and Astronomy, University of St. Andrews, North Haugh, St. Andrews, Fife KY16 9SS, UK*

<sup>3</sup>*Argelander-Institut für Astronomie (Sternwarte), Auf dem Hügel 71, D-53121 Bonn, Germany*

<sup>4</sup>*Institute of Astronomy, Madingley Road, Cambridge CB3 0HA, UK*

Accepted 2008 November 16. Received 2008 November 5; in original form 2008 September 2

## ABSTRACT

The study of young stellar populations has revealed that most stars are in binary or higher order multiple systems. In this study the influence on the stellar initial mass function (IMF) of large quantities of unresolved multiple massive stars is investigated by taking into account stellar evolution and photometrically determined system masses. The models where initial masses are derived from the luminosity and colour of unresolved multiple systems show that even under extreme circumstances (100% binaries or higher order multiples) the difference between the power-law index of the mass function of all stars and the observed mass function is small ( $\lesssim 0.1$ ). Thus, if the observed IMF has the Salpeter index  $\alpha = 2.35$  then the true stellar IMF has an index not flatter than  $\alpha = 2.25$ . Additionally, unresolved multiple systems may hide between 15 and 60% of the underlying true mass of a star cluster. While already a known result, it is important to point out that the presence of a large number of unresolved binaries amongst pre-main-sequence (PMS) stars induces a significant spread in the measured ages of these stars even if there is none. Also, lower-mass stars in a single-age binary-rich cluster appear older than the massive stars by about 0.6 Myr.

**Key words:** binaries: close – binaries: general – stars: early-type – stars: evolution – stars: formation – stars: luminosity function, mass function

## 1 INTRODUCTION

Most late-type stars ( $\lesssim 1M_{\odot}$ ) are born in clusters of binary systems with companion masses distributed randomly from the stellar initial mass function (IMF; Goodwin & Kroupa 2005; Goodwin et al. 2007; Goodwin & Whitworth 2007; Kouwenhoven et al. 2008). Subsequent dynamical encounters in the cluster evolve the stellar population to that observed in the Galactic field (Duquennoy & Mayor 1991; Kroupa 1995a,d,b,c; Kroupa & Bouvier 2003). If massive ( $\gtrsim \text{few } M_{\odot}$ ) stars were also to be born with companions distributed randomly from the IMF, then the vast majority of O stars would have M-dwarf companions while massive equal-mass binaries would be extremely unlikely. For random sampling from a canonical IMF (Weidner & Kroupa 2004) for any O star<sup>1</sup> it would be expected that 0.2% of the companions are O stars ( $m \gtrsim 16M_{\odot}$ ), 2.2% B stars ( $2.7M_{\odot} \lesssim m \lesssim 16M_{\odot}$ ), 2.1% A stars ( $1.7M_{\odot} \lesssim m \lesssim 2.7M_{\odot}$ ), 3.7% F stars ( $1.1M_{\odot} \lesssim m \lesssim 1.7M_{\odot}$ ), 3.4% G stars ( $0.85M_{\odot} \lesssim m \lesssim 1.1M_{\odot}$ ), 12.0% K stars

\* E-mail: Carsten.Weidner@st-andrews.ac.uk

† E-mail: pavel@astro.uni-bonn.de

‡ E-mail: tmasch@astro.uni-bonn.de

<sup>1</sup> The percentages are valid for any given star but if the “companion” is more massive than the primary they would switch places and the ratios would change. If we constrain ourselves to O stars as primaries it does not matter if the companion is more massive than the primary because they would be both O stars.

( $0.5M_{\odot} \lesssim m \lesssim 0.85M_{\odot}$ ) and 76.3% M stars ( $0.08 M_{\odot} \lesssim m \lesssim 0.5M_{\odot}$ ). These M-dwarfs (as well as the K and at least the G stars, altogether more than 90% of all companions) would be more or less invisible. However, the observed fraction of O stars in *massive* multiple systems lies between at least 20 and 80% (Garmany et al. 1980; García & Mermilliod 2001; De Becker et al. 2006; Kiminki et al. 2007; Lucy 2006; Apai et al. 2007; Sana et al. 2008; Kouwenhoven et al. 2007; Turner et al. 2008) and thus strongly contradicts secondaries which are randomly taken from the IMF, at least for massive primaries. Unfortunately, the mass ratio ( $q = \frac{m_{\text{secondary}}}{m_{\text{primary}}}$ ) distribution<sup>2</sup> for massive stars is observationally not well explored for several reasons: Massive stars have very broad spectral lines, making radial velocity studies a challenge. Even rather massive and close companions are easy to miss. And young stellar nurseries are usually deeply embedded in gas and dust. Furthermore, massive stars are predominately found in massive clusters. So the issue of crowding and fast dynamical evolution arises and therefore it is not clear if the  $q$ -distribution is primordial. As massive stars either sink to the centre of star clusters through energy equipartition (Grebel 2005; Stolte et al. 2006; Fleck et al. 2006; Vesperini et al. 2006; Zhao et al. 2006) or are (exclusively?) formed there (Bonnell et al. 1998, 2003, 2004), dynamical processes in the cluster centre can expel (massive) stars from the cluster and/or exchange binary partners, thereby changing the  $q$ -distribution (Pflamm-Altenburg & Kroupa 2006; Pfalzner & Olczak 2007). This picture is strongly supported by the fact that “field” and runaway O stars have a far lower binary fraction than O stars in clusters and associations (Turner et al. 2008; Mason et al. 2008). A recent study of triple and quadruple system by Tokovinin (2008) might also be used as an argument against random pairing of stars as the author finds a surprisingly large amount of these systems in which all stars are of similar mass. Whether or not these results are applicable to this study is a matter of debate. The Tokovinin (2008) sample consists to about 80% of primary stars below  $5 M_{\odot}$  and it is not restricted to young objects. If the author’s claim is correct that properties like orbital periods and eccentricities of old multiple systems are not consistent with  $N$ -body calculations his study would be an important argument against random pairing of multiple stars. It should be noted here that in a cluster of the richness of the Orion Nebula cluster stellar dynamics may change the mass function and binary properties in the core significantly in less than  $10^6$  yr (Pflamm-Altenburg & Kroupa 2006; Pfalzner & Olczak 2007). The study of the  $q$ -distribution in the present paper is of stars at the stage when they are observed and may thus be representative of dynamically evolved distributions.

The influence of a substantial fraction of unresolved binary systems on the low-mass stellar mass function (MF) has been well explored (Sagar & Richtler 1991; Kroupa et al. 1991, 1993; Kroupa 1995a,d; Malkov & Zinnecker 2001; Thies & Kroupa 2007, 2008). Beginning from the lowest mass stars and brown dwarfs, Thies & Kroupa (2007, 2008) corrected for un-resolved companions in such systems and showed that the IMF is discontinuous near  $0.1 M_{\odot}$ . In an extensive study of late-type stars, Kroupa et al. (1991, 1993) showed that the mass function of these stars is significantly affected by unresolved systems. They used this result to formulate the standard or canonical-IMF with little or no evidence for systematic variations with star forming conditions (Kroupa 2001, for more details on the canonical IMF: see Appendix A). Interestingly, there seems now to be strong evidence for a universal companion mass function for solar type stars (Metchev & Hillenbrand 2008). But only a very limited number of studies have addressed how the large proportion of binaries affects IMF derivations for massive stars. Sagar & Richtler (1991) studied the MFs of five young star clusters in the Large Magellanic Cloud (LMC) including the influence of optical and physical binaries on the derived slope of the MFs in the range of  $2\text{--}14 M_{\odot}$  by Monte Carlo simulations of cluster and field populations with random pairing over this mass interval. They found a very strong steepening of the observed MF in the case of a binary fraction larger than 50%. Vanbeveren (1982) investigated the IMF of primaries and single stars analytically up to stars above  $100 M_{\odot}$  but did not explicitly discuss any possible effects of unresolved binaries on the observed IMF. Only rather recently, the study by Maíz Apellániz (2008) explores the biases on the IMF introduced by unresolved binaries for massive stars. There a different colour is used ( $U - V$ ) while in this contribution we resort to  $B - V$ , and only random pairing is studied by Maíz Apellániz (2008, see § 2.1 for details on binary pairing) while here we consider different viable  $q$ -distributions. This contribution can therefore be seen as an extension of these previous studies (Kroupa et al. 1991, 1993; Sagar & Richtler 1991; Malkov & Zinnecker 2001; Thies & Kroupa 2007, 2008) to higher masses as well as a comparison to the Maíz Apellániz (2008) study.

## 2 THE MODEL

In what follows,  $dN = \xi(m) dm$  is the number of stars in the mass interval  $m$  to  $m + dm$ .

For all methods the IMF,  $\xi(m)$ , described in Appendix A is used as the input IMF. For every model the percentage of binaries, triples and quadruples is assigned as an initial condition and then one of the following pairing algorithms is used to obtain the masses of the stars. The primary, secondary etc. is always the most-massive, second massive, etc., companion.

<sup>2</sup> The  $q$ -distribution for random pairing is roughly flat, showing little preference for any particular  $q$ -value (Kroupa 1995c; Grether & Lineweaver 2006).

## 2.1 Pairing algorithms

As the initial properties of (massive) binaries and higher-order multiple systems are generally unknown, several different methods of pairing stars were used.

- Random pairing (RP): A given number of stars is taken fully randomly from the input IMF over the mass range of 0.08 to  $150 M_{\odot}$  and randomly assigned to pairs or higher-order multiple systems.
- Special pairing (SpP): Again a given number of stars is taken randomly from the input IMF over the mass range of 0.08 to  $150 M_{\odot}$  and randomly grouped together. But in the cases where the primary exceeds  $2 M_{\odot}$  the secondary has to fulfil a minimum mass criterion as described in Appendix B1. If the secondary fails this test it is exchanged with another star from the random list until the minimum mass is reached or exceeded. In the case that the new secondary is more massive than the primary the two exchange places and the secondary becomes the new primary and the old one the new secondary. This new secondary still has to fulfil the minimum mass criteria or it is exchanged with another star. It is possible that no such secondary is available in the list anymore. Then the minimum mass is lowered by 20% and if this is still insufficient, the star is kept as a single. In the numerical experiments presented here no such case was encountered. In the case of triple or quadruple systems, if the secondary component is also larger than  $2 M_{\odot}$  the tertiary component is searched for with the same criterion as the secondary before (ie the secondary is treated as the “primary” in the secondary-tertiary sub-system). The same procedure is extended to the quaternary companions (ie. the quaternary becomes the “secondary” of the tertiary).
- System pairing (SyP): A given number of *system* masses is randomly taken from an input (not the canonical) IMF with  $0.16 \leq m_{\text{sys}} \leq 300 M_{\odot}$  and with a change of slope from 1.3 to 2.35 at  $1 M_{\odot}$  instead of  $0.5 M_{\odot}$ . The lower and upper mass limit for *stars* is always kept at 0.08 and  $150 M_{\odot}$ . If the system mass is below  $10 M_{\odot}$  the system is randomly split into two, three or four components assuming a uniform mass-ratio distribution being equivalent to random pairing on this mass interval. But for systems with a mass that exceeds  $10 M_{\odot}$  the  $q$ -values used to split the systems into components are biased towards high- $q$ -values as described in Appendix B2. This model is motivated by a possible merger-origin of massive stars but could also represent the outcome of the competitive accretion model (Bonnell et al. 1998). In order to have a smooth transition between the random mass ratios and the preferential formation of massive companions for the SyP model the change is necessary at  $10 M_{\odot}$  and not at  $2 M_{\odot}$  as in the case of the SpP model.

All pairing mechanisms preserve a lower mass limit of  $0.08 M_{\odot}$  for all components, because stars and brown dwarfs rarely pair up (Thies & Kroupa 2007, 2008).

After the stars are assigned into their systems, the mass function for all stars, for the primaries, secondaries, tertiaries (if applicable) and quaternaries (if applicable) is calculated along with the IMF for the systems. The method used to measure the slopes is presented in § 2.3. The direct results of these calculations are presented in § 3.1 while the calculations additionally applying stellar evolution (as described in § 2.2) are discussed in § 3.2.

## 2.2 Stellar evolution

Stellar observations usually do not result directly in stellar masses and ages but magnitudes and colours. Therefore, the stars produced by the pairing mechanisms described in Section 2.1 are assigned a random age with a Gaussian distribution between 0.01 and 4.5 Myr with a median of 2 Myr and a dispersion of 0.5 Myr. Stars in the same multiple system are assumed to be coeval. Using a large grid of stellar models<sup>3</sup> this age is then used to evolve the stars and obtain the evolved masses, effective temperatures and radii. These values are further used to calculate the Johnson V and B band magnitudes with the help of Kurucz (1992) and Bergeron et al. (1995) bolometric corrections using a program kindly provided by J. Hurley (see Hurley 2003). The luminosities of the individual stars are then combined to a single V magnitude and  $B - V$  colour of the unresolved multiple and searched for in a large table of V and  $B - V$  values made with the same models but for truly single stars and with an age range between 0.01 and 100 Myr<sup>4</sup>. In this manner so-called *pseudo masses* and *pseudo ages* for the unresolved multiples are derived as if they were single stars. Note that the derived *pseudo masses* are the *zero-age* masses.

Note that photometric mass and age determination is known to be inaccurate in comparison to spectroscopic measurements (Massey 2003). But as spectra are far more expensive in terms of observational time the photometric method is still widely in use. Furthermore, for OB stars a spectroscopic analysis does not automatically solve the problem of un-resolved multiples as O stars have very broad lines which easily hide even massive companions. Only with elaborate multi-epoch spectroscopic observations solid constraints can be put on the multiplicity of O stars (Sana et al. 2008; Schnurr et al. 2008).

<sup>3</sup> Meynet & Maeder (2003) models for massive stars, Hurley et al. (2000) for the evolution after the pre-main sequence (PMS) for stars below  $9 M_{\odot}$  and Burrows et al. (1993), Burrows et al. (1997), D’Antona & Mazzitelli (1997), D’Antona & Mazzitelli (1998) and Behrend & Maeder (2001) for PMS evolution. For further details on the used models for stellar evolution see Weidner et al. (2008).

<sup>4</sup> A larger age than the input age of 4.5 Myr is used to additionally show the effect of unresolved multiples on the age determination of stars.

**Table 1.** Standard deviation and bias for the estimation method of the exponent, for different sample sizes and output exponents.

Standard deviation			
# stars	$\alpha = 1.5$	$\alpha = 2.3$	$\alpha = 5.0$
$10^3$	0.026	0.043	0.127
$10^4$	0.009	0.014	0.042
$10^5$	0.003	0.004	0.012
Bias			
# stars	$\alpha = 1.5$	$\alpha = 2.3$	$\alpha = 5.0$
$10^3$	$3 \times 10^{-4}$	$3 \times 10^{-3}$	$1 \times 10^{-2}$
$10^4$	$4 \times 10^{-5}$	$3 \times 10^{-4}$	$2 \times 10^{-3}$
$10^5$	$1 \times 10^{-5}$	$3 \times 10^{-5}$	$1 \times 10^{-4}$

### 2.3 A bias-free fitting method

The common method to analyse power-law distributed data is to group them in bins of constant logarithmic size and then perform a linear regression to measure the power-law index  $\alpha$ . However, this method can lead to strongly biased results (Maíz Apellániz & Úbeda 2005). Therefore here the method of Maschberger & Kroupa (2008) is used. It is based on the estimates for  $\alpha$  obtained with the maximum likelihood method.

The maximum likelihood estimate of the power-law exponent (see Aban et al. 2006) is calculated by minimising the logarithmic likelihood function of the data  $\{X_i\}_{i=1}^n$ , where  $X_i = m_i$  is the mass of star  $i$ . The estimated exponent  $\alpha_{ML}$  is then the solution of

$$-\frac{n}{1 - \alpha_{ML}} + n \frac{Z^{1-\alpha_{ML}} \log Z - Y^{1-\alpha_{ML}} \log Y}{Z^{1-\alpha_{ML}} - Y^{1-\alpha_{ML}}} - T = 0, \quad (1)$$

with the smallest data point,  $Y = \min X_i$ , the largest data point,  $Z = \max X_i$ , and the sum of the logarithms of all data,  $T = \sum_{i=1}^n \log X_i$ . The bias-free estimate follows with

$$\alpha = \frac{n}{n-2}(\alpha_{ML} - 1) + 1. \quad (2)$$

The standard deviation and bias of the method were investigated by using a Monte-Carlo sample of 1000 synthetic data sets, generated with a lower limit of  $1.3 M_{\odot}$ , an upper limit of  $150 M_{\odot}$ , different sizes of the data set and different exponents. For each data set the exponent was estimated and from the sample of estimates the standard deviation and the bias (difference between the average of the estimated exponents and the input value) were calculated. The results are summarised in Table 1. The bias is in all cases negligible. The standard deviation decreases with increasing size of the data set and increases with increasing exponent. For the sample sizes used in this work a conservative estimate of the standard deviation is 0.05.

## 3 RESULTS

In § 3.1 the results of simulating binaries, triples and quadruples are described under the assumption that all stellar masses are known perfectly. In § 3.2 the stars are evolved with the use of stellar evolution models and the combined magnitudes and colours are used to model the process of observing stellar populations containing unresolved multiple systems.

### 3.1 Models without stellar evolution

Shown in Tab. 2 are the parameters and results for a series of models. A number of abbreviations are used in the Table. “100% bin” marks models made of 100% binaries, “100% trip” are 100% triples and “100% quad” are 100% quadruples. The corresponding IMF slopes are:  $\alpha_{\text{allstars}}$ <sup>5</sup> which accounts for all stars individually (ie. the true single-star IMF),  $\alpha_{\text{systems}}$  which is the mass function for the combined masses of all multiple systems,  $\alpha_{\text{primaries}}$  which is the IMF of the most massive component of a system,  $\alpha_{\text{secondaries}}$  for the second most massive component of a system,  $\alpha_{\text{tertiaries}}$  for the third massive object (only in triples and quadruplets) and finally  $\alpha_{\text{quartiaries}}$  for the fourth component in a system if there is any (only quadruplets).

All models are calculated without stellar evolution, meaning they are treated as if all masses are known precisely. For each model  $10^7$  stars are generated, each model taking only about a few minutes of computational time on a standard desktop PC.

<sup>5</sup> All IMF slopes in this work are obtained by a bias-free fitting method discussed in § 2.3 for all stars above  $1 M_{\odot}$ . In the case of strong non-linear features in the MFs the line was fitted to the stars above such features. The standard deviation in  $\alpha$  is of the order of 0.05 dex.

**Table 2.** Properties of the models without stellar evolution. The pairing methods are described in Section 2.1. All stars are in 100% binaries, triples or quadruples, respectively. The slopes are measured by the bias-free method (see § 2.3) above  $1.0 M_{\odot}$  unless noted otherwise. For each model a total of  $10^7$  stars are generated. Column #1 denotes the model name, #2 the pairing method, #3 if the systems are binaries, triples or quadruples, #4 shows the slope for all stars, #5 the slope of the systems, #6 the slope of the primaries, #7 the slope of the secondaries, #8 the slope of the tertiaries and #9 the slope of the quartaries.

Model	pairing method	multiple	$\alpha_{\text{allstars}}$	$\alpha_{\text{systems}}$	$\alpha_{\text{primaries}}$	$\alpha_{\text{secondaries}}$	$\alpha_{\text{tertiaries}}$	$\alpha_{\text{quartaries}}$
1	RP	bin	2.35	2.40 <sup>1</sup>	2.32	3.71	-	-
2	RP	trip	2.35	2.47 <sup>1</sup>	2.28	3.64	5.14	-
3	RP	quad	2.35	2.54 <sup>1</sup>	2.26	3.60	4.96	6.06
4	SpP	bin	2.35	2.34 <sup>1</sup>	2.36	2.04 <sup>2</sup>	-	-
5	SpP	trip	2.35	2.38 <sup>1</sup>	2.34	2.13 <sup>2</sup>	1.93	-
6	SpP	quad	2.35	2.42 <sup>1</sup>	2.31	2.22 <sup>2</sup>	1.78 <sup>2</sup>	1.62 <sup>2</sup>
7	SyP	bin	2.35	2.35	2.60 <sup>1</sup>	2.27	-	-
8	SyP	trip	2.35	2.35	2.57 <sup>1</sup>	2.26	2.25	-
9	SyP	quad	2.35	2.35	2.55 <sup>1</sup>	2.25	2.25	2.25
10	q=1	bin	2.35 <sup>1</sup>	2.35 <sup>1</sup>	2.32	2.36 <sup>1</sup>	-	-

<sup>1</sup> slope measured above  $10.0 M_{\odot}$ , <sup>2</sup> slope measured above  $2.0 M_{\odot}$

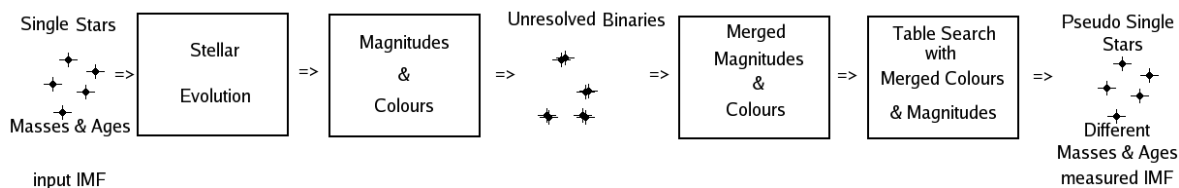


**Figure 1.** Stylised flow chart how stellar evolution and unresolved binaries influence the observed mass function.

As is seen in Tab. 2 and the first three panels of Fig. C1 the models using random sampling (RP Model 1 to 3) produce system IMFs which are somewhat steeper than the input IMF, and very steep IMFs for the companions, while the primary IMFs are slightly flatter. This can be understood as due to random pairing producing systems in which most of the massive stars have low-mass companions. These do not change the mass of the system significantly. But the low-mass systems tend to have partners of very similar mass, therefore additionally depleting the total number of low-mass systems and shifting them to higher masses.

The special pairing mechanism explored here (SpP Model 4 to 6) has a different effect. The system IMF is also steepened but only for the case of 100% quadruples (SpP Model 6) and the companion star IMFs are flattened below the Salpeter-value for the secondaries, tertiaries and quartaries for all three models. But for the primaries the IMF becomes slightly steeper. In the panels 4, 5 and 6 of Figs. C1 and C2 this can be seen. This is expected since the SpP mechanism searches for massive companions for massive stars and therefore depletes the reservoir of massive stars remaining as primaries, and in doing so channels large amounts of massive stars into the companion star IMFs.

A similar, but even more drastic result is obtained by system pairing (SyP Models 7 to 9, panels 7 to 9 in Figs. C2 and C3). Here the primary IMFs are steepened and the secondary IMFs flattened in order to retain constant slopes for the system IMFs under the condition of having increasingly higher  $q$ -values for more massive systems.

The rather flat slopes of the companion mass functions for SpP and SyP would be in agreement with the results of Tokovinin (2008) that for a large fraction of triple and quadruple systems the components are of rather similar mass.

For reasons of comparison also an example of 100% equal-mass binaries for massive stars (for primaries  $> 2 M_{\odot}$ ) is shown (Model 10 in Tab. 2 and panel 10 in Fig. C3). Here in principle all IMFs are parallel but again discontinuous features appear in the IMFs at the borders of the random pairing for the low-mass stars and the  $q = 1$  pairing for the more massive ones.

### 3.2 Models with stellar evolution

In a second set of models the influence of the conversion of luminosities into masses is studied. The systems have ages assigned from a Gaussian distribution with a mean of 2 Myr and a standard deviation of 0.5 Myr and a cutoff at 0.01 and 4.5 Myr. With this age the stars are evolved according to the models described in Section 2.2. The resulting stellar parameters are used to calculate luminosities and colours for each single star. These are merged to form an unresolved multiple system ensuring coevality of all companions. The resulting magnitudes and colours are searched for in a large table of colours/magnitudes of

**Table 3.** Like Tab. 2 but for the models with stellar evolution. For each model a total of 1 million stars are generated. Column #1 (model) denotes the model name, #2 (pairing method) the pairing method, #3 (multiple) if the systems are binaries, triples or quadruples, #4 ( $\alpha_{\text{allstars}}$ ) shows the IMF slope for all stars above  $1 M_{\odot}$ , #5 ( $\alpha_{\text{systems}}$ ) the slope of the systems, #6 ( $\alpha_{\text{prim}}$ ) the slope of the primaries, #7 ( $\alpha_{\text{sec}}$ ) the slope of the secondaries, #8 ( $\alpha_{\text{tert}}$ ) the slope of the tertiaries, #9 ( $\alpha_{\text{quart}}$ ) the slope of the quartiaries, #10 ( $\alpha_{\text{observed}}$ ) the slope of the recovered “observed” stars, #11 (age fit) marks the percentage for how many of the unresolved stars the pseudo age of the system is recovered within 25% of the original age, #12 (total mass recovered) shows the percentage of the input mass in stars which was recovered in “observed” stars and #12 (age fit mass) is the recovered mass in stars for which the pseudo ages are within 25% of the real ages. The differences in the values for the slopes of the primaries, secondaries, tertiaries and quartiaries in comparison with Tab. 2 are due to the lower number of stars used for the models with stellar evolution, as these lower numbers significantly increase the error of the slope determination.

Model	pairing method	multiple	$\alpha_{\text{allstars}}$	$\alpha_{\text{systems}}$	$\alpha_{\text{prim}}$	$\alpha_{\text{sec}}$	$\alpha_{\text{tert}}$	$\alpha_{\text{quart}}$	$\alpha_{\text{observed}}$	age fit	total mass recovered	age fit mass
Fit 0 <sup>1</sup>	RP	bin	2.35	2.40 <sup>2</sup>	2.32	3.71	-	-	2.36 <sup>2</sup>	50%	84%	59%
Fit 1	RP	bin	2.35	2.40 <sup>2</sup>	2.32	3.70	-	-	2.35 <sup>3</sup>	50%	85%	43%
Fit 2	RP	trip	2.35	2.47 <sup>2</sup>	2.29	3.63	5.11	-	2.34 <sup>3</sup>	34%	73%	43%
Fit 3	RP	quad	2.35	2.54 <sup>2</sup>	2.25	3.62	4.98	6.08	2.33 <sup>3</sup>	25%	65%	33%
Fit 4	SpP	bin	2.35	2.36 <sup>2</sup>	2.37	2.07 <sup>3</sup>	-	-	2.43 <sup>3</sup>	49%	80%	44%
Fit 5	SpP	trip	2.35	2.36 <sup>2</sup>	2.34	2.15 <sup>3</sup>	1.98	-	2.42 <sup>3</sup>	32%	68%	30%
Fit 6	SpP	quad	2.35	2.40 <sup>2</sup>	2.32	2.22 <sup>3</sup>	1.83 <sup>3</sup>	1.67 <sup>3</sup>	2.43 <sup>3</sup>	23%	60%	23%
Fit 7	SyP	bin	2.35	2.35	2.60 <sup>2</sup>	2.26	-	-	2.41 <sup>2</sup>	43%	70%	25%
Fit 8	SyP	trip	2.35	2.35	2.56 <sup>2</sup>	2.25	2.24	-	2.46 <sup>2</sup>	22%	53%	10%
Fit 9	SyP	quad	2.35	2.35	2.54 <sup>2</sup>	2.25	2.25	2.23	2.43 <sup>2</sup>	19%	43%	5%
Fit 10	q=1	bin	2.35 <sup>2</sup>	2.35 <sup>2</sup>	2.31	2.37 <sup>2</sup>	-	-	2.31 <sup>2</sup>	45%	68%	10%

<sup>1</sup> This model is included for comparison only. It is identical to Fit 1 but all stars have a fixed input age of 2 Myr instead of the Gaussian distributed ages for the other models.

<sup>2</sup> slope measured above  $10.0 M_{\odot}$ , <sup>3</sup> slope measured above  $2.0 M_{\odot}$

single stars produced with the use of the same models as in Section 2.2 in order to find a *pseudo zero-age mass* and a *pseudo age* for the unresolved multiple as if it were a single star. The table covers a mass range between  $0.01 M_{\odot}$  and  $300 M_{\odot}$  with ages between zero and 100 Myr. In Fig. 1 the steps described above are visualised. As this procedure is rather CPU time consuming only 1 million stars are generated for each model in contrast to the 10 million in Section 3.1. Each model needs about 27 hours of CPU time on a state-of-the-art PC.

The results and parameters for this second series of models are listed in Tab. 3. Additionally to the columns shown in Tab. 2  $\alpha_{\text{observed}}$  is added: the IMF slope of the mass function for all unresolved systems above  $1 M_{\odot}$  recovered by the simulated observations. In some models strong non-linear features occur in the output close to  $1 M_{\odot}$ . In such cases a higher lower limit for the slope determination is used as indicated in the Table. The slope is determined in the same way as in § 3.1. Furthermore, included is the column “age fit” in Tab. 3 which is the percentage of how many pseudo stars are recovered with a pseudo age within 25% of the real age of the system. Finally, the last two columns contain the recovered total mass fraction and the recovered mass fraction within the 25% age limit. In the first case the total mass of all recovered pseudo stars for one model is divided by the true stellar mass within the model and in the second case only the pseudo mass of the recovered pseudo stars with pseudo ages within 25% of their real ages is divided by the total true mass. Furthermore, for reasons of comparison, Model Fit 0 is only included in Tab. 3 but not otherwise used. This model is similar to Model Fit 1 in all aspects but the age. Instead of an age spread all stars have the same input age of 2 Myr.

Because of the fewer stars used here in comparison with § 3.1 the errors in the slope determination are larger than in the previous experiments without stellar evolution.

In the first panel of Fig. D1 (Model Fit 1, random pairing, 100% binaries, see also the exemplary HR-Diagrams for this model in Fig. 2) the input, primary, secondary and system IMF are the same as for Model 1 from Section 3.1 but with a larger scatter because of the smaller number of generated stars. The derived observed IMF does not follow the (slightly) steeper system IMF but follows instead the input IMF of all stars. The steeping effect seen in the system IMF in comparison to the IMF of all stars is thus fully negated. This is due to the fact that while in the model without stellar evolution all masses are 100% accounted for, in this model with evolution the low-mass companions of massive stars are “lost” because the primary dominates the light and only its mass is recovered. In the low-mass regime all stars are of rather similar mass and therefore the unresolved binaries change the luminosity of the system but not the  $(B - V)$  colour. This makes them appear as younger PMS stars, usually rather close to the mass of the primary. Both model series with mass-dependent mass-ratios (SpP and SyP, panels 4 to 9 in Figs. D2 and D3) have slightly steeper observed IMFs with a slope of about 2.45. But such a small deviation from the Salpeter-slope is within the error margin of measured high-mass IMF slopes. The final Model Fit 10 in which all

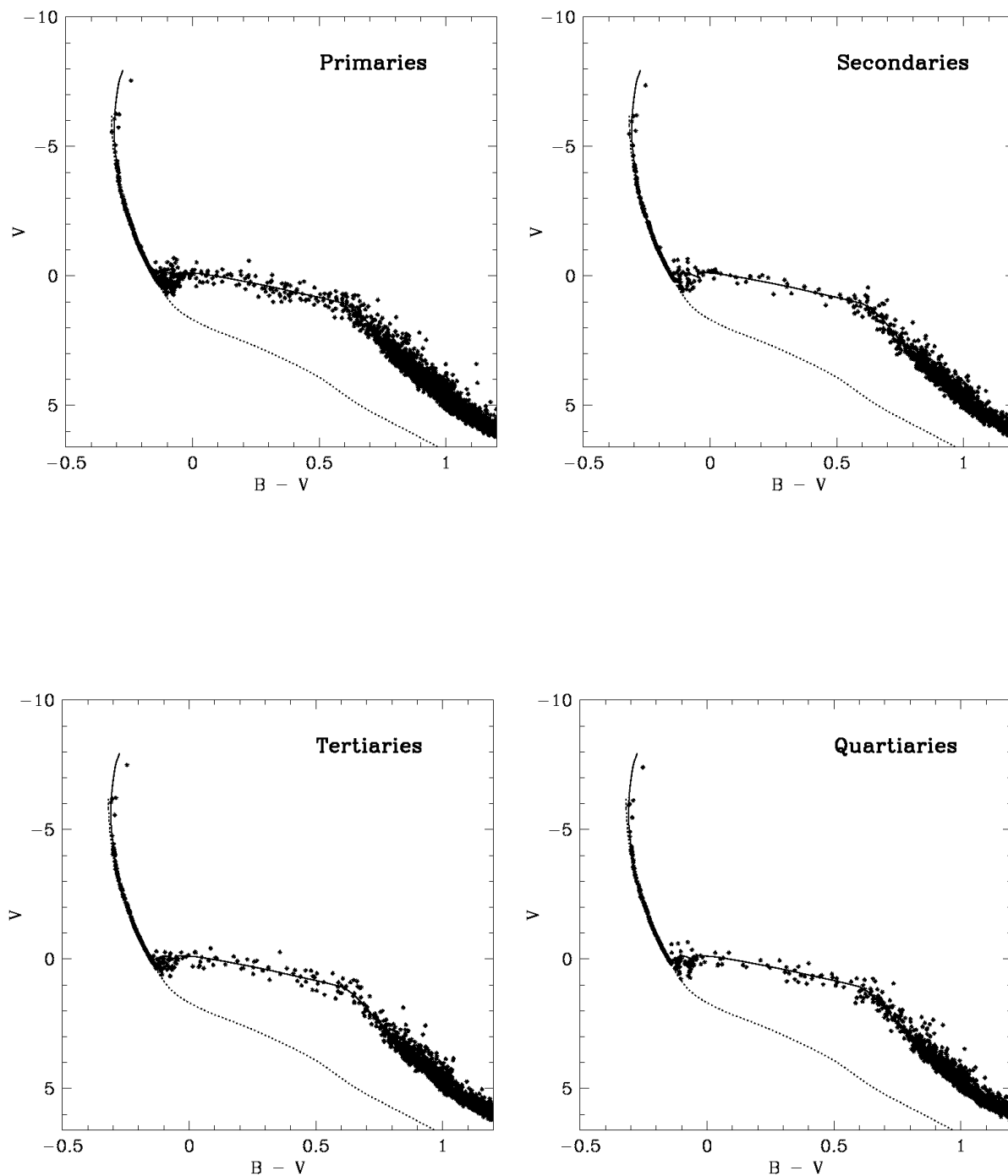


**Figure 2.** HR-Diagrams for the primaries, secondaries, tertiaries and quartaries stars for 17000 stars from model Fit 9. The *solid line* is a 2 Myr isochrone while the *dotted line* is a zero-age main-sequence.

stars above  $2 M_{\odot}$  reside in equal mass binaries influences the slope of the primary IMF and the observed IMF slightly. But such small differences ( $\Delta\alpha = 0.04$ ) are still within the errors of the here used slope determinations.

In conclusion, the analysis presented here quite clearly shows that the observed IMF for massive stars remains mostly indistinguishable from the underlying true stellar IMF, which may be flatter by at most  $\Delta\alpha = 0.1$  even if all massive stars reside in quadruple systems. This would thus indicate that measured IMF indices are quite robust and that the Salpeter/Massey slope,  $\alpha = 2.35$ , is not significantly affected by unresolved multiple stars above a few  $M_{\odot}$ .

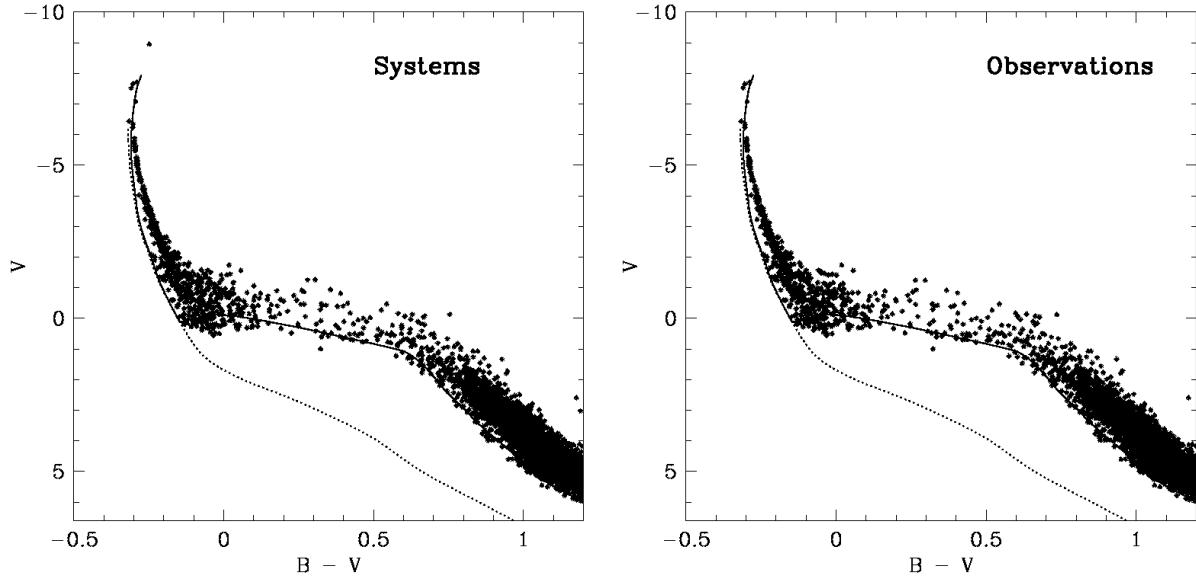


**Figure 3.** HR-Diagrams for the systems and the observed pseudo stars for 17000 stars from model Fit 9. The *solid line* is a 2 Myr isochrone while the *dotted line* is a zero-age main-sequence.

**Table 4.** Percentages of recovered ages in different age bins for a number of models.

Model	< 0.5 Myr	0.5 - 1.5 Myr	1.5 - 5.0 Myr	5.0 - 10.0 Myr	10 <sup>+</sup> Myr
random ages (like Fit 1 to Fit 10),					
50% bin RP	1.5	19.7	74.1	1.6	3.1
0.5 Myr, 100% bin RP	58.5	22.1	11.5	3.5	4.4
1.0 Myr, 100% bin RP	8.0	65.2	10.3	9.0	7.5
2.0 Myr, 100% bin RP	4.8	28.9	53.0	4.3	9.0
3.0 Myr, 100% bin RP	3.0	10.3	75.0	4.8	7.0
Fit 1	4.4	31.8	50.0	4.6	9.1
Fit 4	4.4	31.8	49.3	4.9	9.5
Fit 7	5.3	38.0	41.9	3.8	11.1
Fit 10	4.7	33.9	45.0	4.7	11.5

### 3.2.1 Age spreads

Interestingly, as is seen in the ninth column of Tab. 3, only about 40 to 50% of the pseudo stars are recovered with the right pseudo age (with an error of less than 25% compared to the true age). Actually, the discrepancy between assigned age and fitted age can be rather large. Therefore, large numbers of binaries (regardless of their masses) can mimic a wide spread of formation ages. In order to further explore this interesting result a series of models is calculated with  $5 \cdot 10^5$  binaries (0.08 to 150  $M_{\odot}$  for the stars), random pairing and the same input age. The distribution of the resulting recovered ages (using the same method as before in § 3.2) for stars of all masses can be seen in Figs. 4 to 7. Fig. 4 features an input age of 0.5 Myr, Fig. 5 1 Myr, Fig. 6 2 Myr and Fig. 7 3 Myr.

Using such a single input age (e.g. 1 Myr) as in Fig. 5 the distribution of the recovered output ages is severely distorted (*dotted histogram* in Fig. 5). In Tab. 4 are shown the percentages of recovered ages in several age bins. Besides the models with single input ages also the Models Fit 1, Fit 4, Fit 7 and Fit 10 are included as well as a model with only 50% binaries and the same age range as the Models Fit 1 to Fit 10.

In a real star cluster it is unlikely that all stars are truly of the same age. Therefore in Fig. 8 a distribution of input ages is used. Fig. 8 shows as an example the age distribution for Model Fit 1. While the *solid histogram* is the Gaussian input age distribution (distorted because of the logarithmic ordinate), the *dotted histogram* is the recovered age distribution. The mean of the recovered ages of all stars is slightly lower than the true mean age (1.6 Myr instead of 2 Myr). This is consistent with the findings by Brandner & Zinnecker (1997) and Preibisch & Zinnecker (1999) that un-resolved binaries let a population

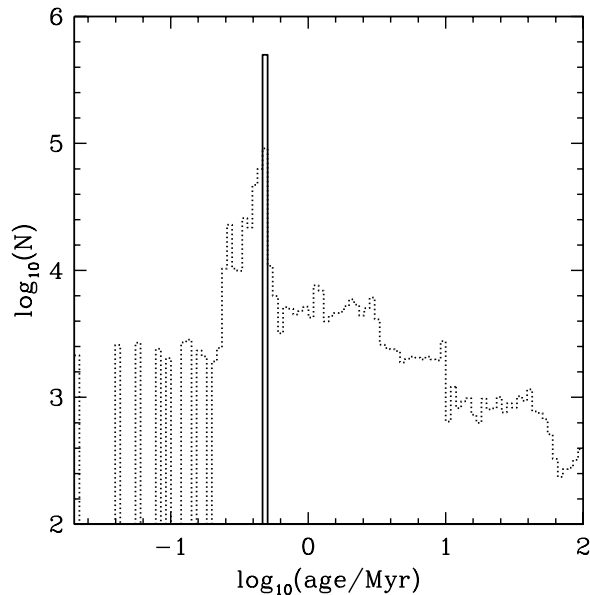


**Figure 4.** Logarithm of the number of stars versus logarithm of the age for one million stars in 100% unresolved RP binaries (500000 systems). *Solid histogram:* The input age of 0.5 Myr. *Dotted histogram:* The recovered output ages for stars of all masses.

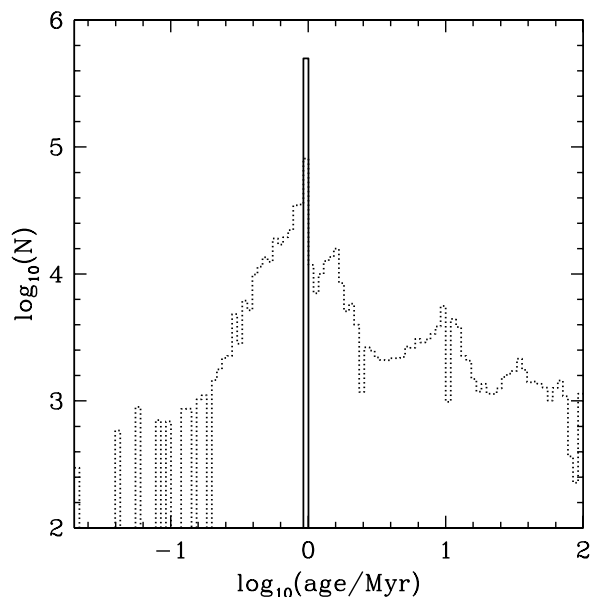


**Figure 5.** Like Fig. 4 but with an input age of 1 Myr.

appear younger than it is. Additionally, the wings of the recovered distribution are much wider - suggesting the presence of stars even up to an age of 100 Myr, despite the maximal input age of about 4.5 Myr. Variability of these PMS stars and photometric errors make the age derivation even more difficult (Briceño et al. 2007; Hillenbrand et al. 2008).

In Fig. 9 the same recovered output ages as in Fig. 8 are shown but split into two, for stars above  $1 M_{\odot}$  (*dotted histogram*) and below (*long-dashed histogram*). It can be seen that the tail towards old ages is prominent in both populations but the tail on the left hand side, towards young ages, is more dominant for low-mass stars. However, the actual peak of the high-mass distribution is moved from 2 Myr to 1 Myr while the low-mass stars peak in between at about 1.6 Myr. The bulk low-mass stellar population therefore *appears older* by 0.6 Myr than the massive stars.

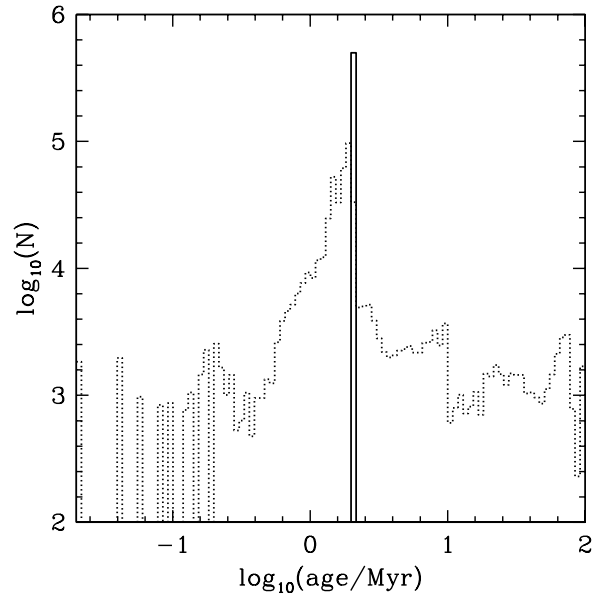


**Figure 6.** Like Fig. 4 but with an input age of 2 Myr.

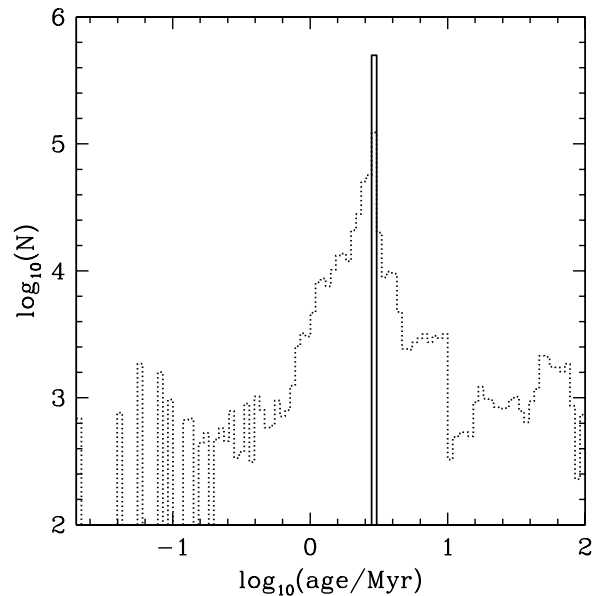


**Figure 7.** Like Fig. 4 but with an input age of 3 Myr.

So, it is important to note that unresolved binaries easily lead to the impression of extended star-formation in a cluster and to the low-mass stars appearing older. Therefore, any age spread encountered in young stellar clusters needs to be interpreted very carefully, as there are also other processes which may masquerade an age spread, e.g. older stars captured during the formation of the star cluster (Fellhauer et al. 2006; Pflamm-Altenburg & Kroupa 2007) and/or unresolved multiple stars as shown here.

Figs. 10 and 11 show some details how the difference in the age determination comes about. The solid line in both figures refers to the evolution of an unresolved binary composed of equal age  $1 M_{\odot}$  and  $0.5 M_{\odot}$  stars using the PMS and main-sequence (MS) tracks as described in Section 2.2. In Fig. 10 the first few Myr are shown. Marked in the figure are also

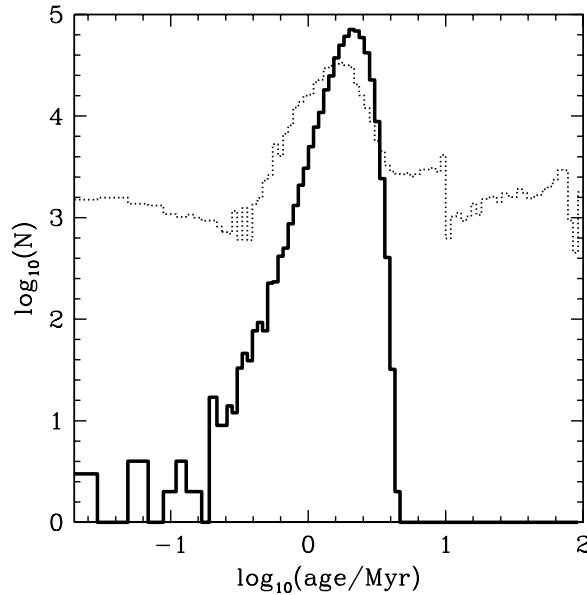


**Figure 8.** Logarithm of the number of stars versus logarithm of the age for Model Fit 1. *Solid histogram:* The assigned input age. *Dotted histogram:* The recovered output age of all stars.

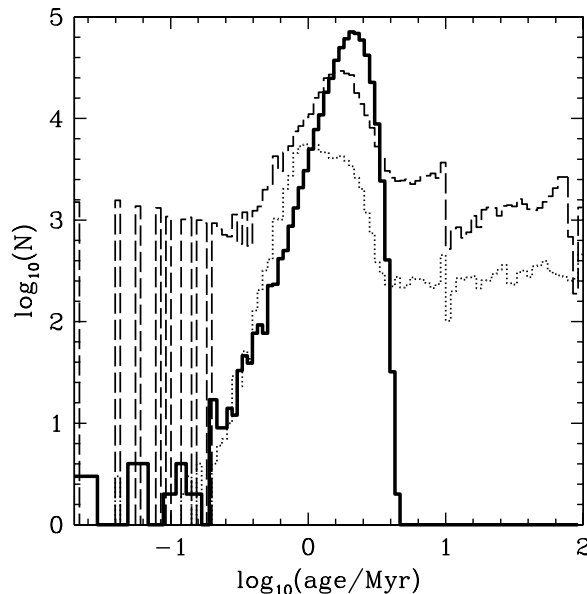


**Figure 9.** Like Fig. 8 but split for high- and low-mass stars. The *dotted line* shows the histogram of output ages for stars above  $1 M_{\odot}$  and the *long-dashed* one for stars below that limit.

the evolutionary tracks for four different single stars. A  $1 M_{\odot}$  star, one of  $1.25 M_{\odot}$ , a  $0.8 M_{\odot}$  and a  $0.5 M_{\odot}$  star. Within its first 1.4 Myr the binary first looks like a  $1.25 M_{\odot}$  star until it evolves parallel for some time to a  $0.8 M_{\odot}$  star. The measured age of the binary is 0.11 Myr when it crosses the  $1 M_{\odot}$  track, while the true age of the two companion stars at that moment is 0.05 Myr. Between 0.3 and 1.4 Myr the binary looks almost identical to a  $0.8 M_{\odot}$  star but this star evolves through this part of its track at an age between 0.16 and 0.66 Myr. Therefore, the binary of  $1.5 M_{\odot}$ , interpreted as a single star, looks for about 1 Myr like a  $0.8 M_{\odot}$  star of only half its age.

In Fig. 11 the final contraction of the pre-main-sequence stars to the zero-age-main-sequence (ZAMS) and the first Myr

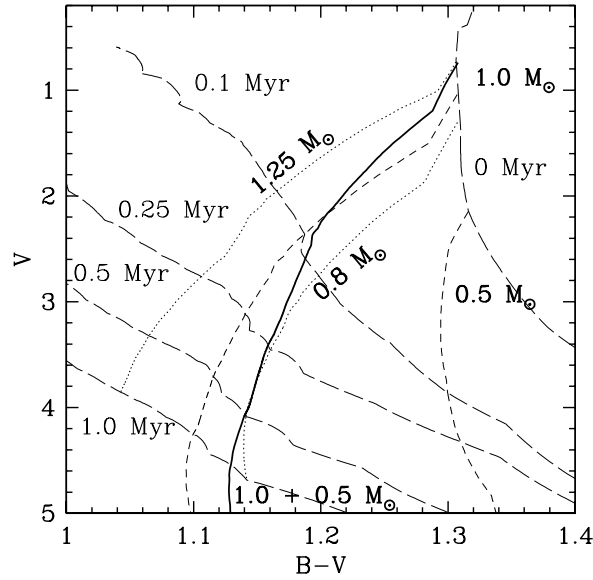


**Figure 10.** The evolution of some young stars through the colour-magnitude diagram along the Hayashi contraction tracks for the first 3 Myr. The *dotted* and *short-dashed lines* indicate the evolution of single stars, while the *thick solid line* shows a binary made of a  $1 M_{\odot}$  and a  $0.5 M_{\odot}$  star. The *thin long-dashed lines* represent isochrones for single stars with ages as indicated in the figure. For more details see the text in § 3.2.1.

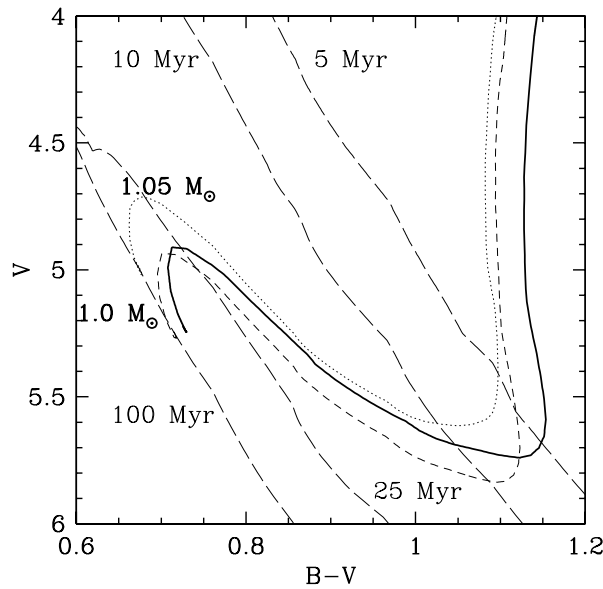


**Figure 11.** Like Fig. 10 but following the PMS evolution until an age of 100 Myr. For details see the text in § 3.2.1.

of the later MS evolution up to an age of 100 Myr is shown<sup>6</sup>. Here the binary evolves for some time parallel to the track of a  $1.05 M_{\odot}$  star. But while the  $1.05 M_{\odot}$  object moves through this phase when 9.5 to 22 Myr old the binary is about 5 Myr older, with a true age between 14 and 25 Myr.

<sup>6</sup> The  $1.05 M_{\odot}$  star needs about 40 Myr to reach the ZAMS while the process takes roughly 80 Myr for the  $1 M_{\odot}$  star.

### 3.3 Recovered total stellar mass

As not all stars are recovered when observing unresolved multiple stars because they are either absorbed in pseudo stars or appear with a pseudo age too different to the bulk age, not only the ages are effected but also the deduced amount of mass in stars in a cluster. The two last columns in Tab. 3 show the fraction of recovered mass in the different models in proportion to the initial mass of the  $10^6$  original stars. First, all the “pseudo” masses for all recovered stars are added up and then divided by the sum of the real masses of all stars in the calculation. And second, only the “pseudo” masses of the stars with pseudo ages recovered within 25% of the real age are added up and compared with the real total mass of all stars. This second comparison is made because in a real observed sample stars with “wrong” ages might not be counted as cluster members but as field stars appearing superposed on the cluster. As can be seen in the second last column between 15 and nearly 60% of the true mass might be missed due to unresolved multiples. If only the stars are considered which are well within the true age of the systems (last column of Tab. 3) between 41 and 95% of the actual mass of the star cluster can be missed. It should be noted here that, as pointed out in § 1, the dynamics of massive stars in star clusters might change the mass-ratios of massive multiple systems towards more massive companions. This would result in an increasing amount of “hidden” mass in the cluster even if all stars were randomly paired in the beginning. This can be seen in Tab. 3 by the fact that both methods, “SpP” and “SyP”, have lower recovered total masses than the “RP” method. Additionally, the unresolved multiple stars can influence dynamical mass estimates of star clusters by biasing radial velocity measurements (Kouwenhoven & de Grijs 2008).

## 4 DISCUSSION AND CONCLUSIONS

A large numerical study has been carried out to determine whether unresolved multiple stars might hide a different underlying massive-star IMF in the observational data. In order to do so three different pairing mechanisms have been considered in order to produce the unresolved systems.

The main difference between these three pairing mechanisms can be summarised as follows: Random Pairing (RP) keeps the MF of all stars and the MF of the primaries constant. As the MF of secondaries is constrained by the input IMF RP changes the system IMF. The “Special Pairing” (SpP) method with its mass-dependent lower mass limit for companions of massive stars keeps all MFs (above  $1M_{\odot}$ ) parallel but changes the system MF in a way similar to RP. As “System Pairing” (SyP) keeps the system MF as a constant input and puts constraints on the mass-ratio for massive systems, the primary and companion MFs are changed to fulfil these constraints.

A first set of models (§ 3.1) has been studied under the assumption that all the masses of the stars and systems can be recovered exactly from the observations. While in the second set (§ 3.2) the stars are evolved according to stellar evolution models, then merged following the different pairing algorithms and retrieved as if they were single stars. The results of this study of the effect of large numbers of unresolved multiple stars can be summarised as follows:

- For random pairing and special pairing the system IMF is always slightly steeper above  $1 M_{\odot}$  than the IMF for all stars (Tab. 2).
- This, however, does not automatically lead to a steeper observed mass function.
- In the case of random sampling there is no effect on the observed IMF above  $1 M_{\odot}$  whatsoever (Tab. 3). This seems to be in contrast with some of the results by Maíz Apellániz (2008). For certain combinations of lower and upper mass limits Maíz Apellániz (2008) find differences in the slopes of up to  $\Delta\alpha = \pm 0.2$ . But when using a similar upper mass limit ( $120 M_{\odot}$ ) as in this study ( $150 M_{\odot}$ ) he finds only very little changes in the slope. He concludes that “in most cases the existence of unresolved binaries has only a small effect on the massive-star IMF slope”. His conclusions are different for chance superpositions of stars which are not considered in this contribution.
- For special pairing and system pairing the observed IMF is slightly steeper ( $\Delta\alpha \approx 0.1$  dex) than the IMF for all stars (see Fig. 12). Therefore, an in reality observed IMF slope of 2.35 therefore might have a true underlying IMF for all stars of 2.25 above a few  $M_{\odot}$ .
- The effect is in general smaller than the error bars on observational slopes of IMFs.
- Nonetheless, unresolved multiple systems can hide between 15% and up to 95% of the mass of a star cluster, depending on the pairing mechanism and the amount of higher order unresolved systems.
- Furthermore, age dating in star clusters can be affected severely:
  - Even a single-age population will appear to have an age spread if the fraction of unresolved multiples is large.
  - Lower mass stars can appear 0.6 Myr older than massive stars in this case.

Based on the broad range of models presented here we conclude that an observed Salpeter/Massey IMF slope ( $\alpha_{\text{obs}} = 2.35$ ) can only mask a slightly flatter IMF for all stars with  $\alpha_{\text{true}} \approx 2.25$ .

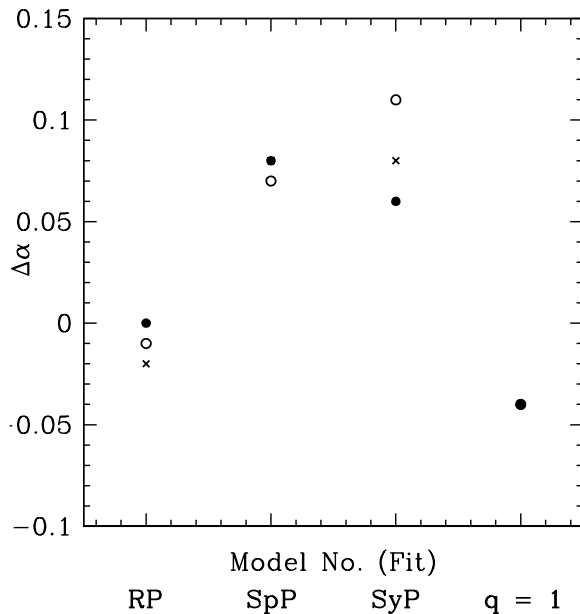


**Figure 12.** Change in slope ( $\Delta\alpha = \alpha_{\text{observed}} - \alpha_{\text{allstars}}$ ) between the observed slope and a slope for all stars of the models with stellar evolution (see Tab. 3). *Filled black dots* indicate models with 100% binaries, *open circles* are the models with 100% triples and the “x”-symbols show models with 100% quadruples. Note that for Model Fit 4 ( $q = 1$ ) only the 100% binary case is shown and that for Model Fit 2 (SpP) the values for the binaries and the quadruples are too close together to be distinguishable.

It should be noted here that Maíz Apellániz (2008) too finds little evidence for effects of unresolved, random paired, binaries on the slope of the IMF of massive stars despite using a different colour ( $U - V$  instead of  $B - V$ ), different stellar evolution models, different routines to calculate the colours and another method to measure the slopes of the mass functions. But he further concludes that chance superpositions of stars in star clusters also introduce a bias on the slope determination, and that the slope-fitting method via histogram construction additionally biases slope determinations (see also Maíz Apellániz & Úbeda 2005). Due to our novel approach by using a bias-free maximum likelihood method (see § 2.3) to measure the slopes of the mass functions we do not suffer from the disadvantages of the histogram fitting method as described in Maíz Apellániz & Úbeda (2005) and Maíz Apellániz (2008).

## ACKNOWLEDGEMENTS

We thank Christopher Tout for helpful discussions and Jarrod Hurley for kindly providing us with his FORTRAN routines for the conversion of luminosities and effective temperatures into magnitudes and colours. Part of this work was financially supported by the Chilean FONDECYT grand 3060096 and the European Commission Marie Curie Research Training Grant CONSTELLATION (MRTN-CT-2006-035890).

## REFERENCES

- Aban I. B., Meerschaert M. M., Panorska A. K., 2006, *Journal of the American Statistical Association*, 101, 270
- Apai D., Bik A., Kaper L., Henning T., Zinnecker H., 2007, *ApJ*, 655, 484
- Behrend R., Maeder A., 2001, *A&A*, 373, 190
- Bell E. F., McIntosh D. H., Katz N., Weinberg M. D., 2003, *ApJS*, 149, 289
- Bergeron P., Wesemael F., Beauchamp A., 1995, *PASP*, 107, 1047
- Bonnell I. A., Bate M. R., Vine S. G., 2003, *MNRAS*, 343, 413
- Bonnell I. A., Bate M. R., Zinnecker H., 1998, *MNRAS*, 298, 93
- Bonnell I. A., Vine S. G., Bate M. R., 2004, *MNRAS*, 349, 735
- Brandner W., Zinnecker H., 1997, *A&A*, 321, 220

- Briceño C., Preibisch T., Sherry W. H., Mamajek E. A., Mathieu R. D., Walter F. M., Zinnecker H., 2007, *Protostars and Planets V*, pp 345–360
- Burrows A., Hubbard W. B., Saumon D., Lunine J. I., 1993, *ApJ*, 406, 158
- Burrows A., Marley M., Hubbard W. B., Lunine J. I., Guillot T., Saumon D., Freedman R., Sudarsky D., Sharp C., 1997, *ApJ*, 491, 856
- Chabrier G., 2003, *PASP*, 115, 763
- Dabringhausen J., Hilker M., Kroupa P., 2008, *MNRAS*, 386, 864
- D’Antona F., Mazzitelli I., 1997, *Memorie della Societa Astronomica Italiana*, 68, 807
- D’Antona F., Mazzitelli I., 1998, in Rebolo R., Martin E. L., Zapatero Osorio M. R., eds, *ASP Conf. Ser. 134: Brown Dwarfs and Extrasolar Planets A Role for Superadiabatic Convection in Low Mass Structures?*. pp 442–+
- De Becker M., Rauw G., Manfroid J., Eenens P., 2006, *A&A*, 456, 1121
- Duquennoy A., Mayor M., 1991, *A&A*, 248, 485
- Elmegreen B. G., 1999, *ApJ*, 515, 323
- Fellhauer M., Kroupa P., Evans N. W., 2006, *MNRAS*, 372, 338
- Figer D. F., 2005, *Nature*, 434, 192
- Fleck J.-J., Boily C. M., Lançon A., Deiters S., 2006, *MNRAS*, 369, 1392
- García B., Mermilliod J. C., 2001, *A&A*, 368, 122
- Garmany C. D., Conti P. S., Massey P., 1980, *ApJ*, 242, 1063
- Goodwin S. P., Kroupa P., 2005, *A&A*, 439, 565
- Goodwin S. P., Kroupa P., Goodman A., Burkert A., 2007, in Reipurth B., Jewitt D., Keil K., eds, *Protostars and Planets V The Fragmentation of Cores and the Initial Binary Population*. pp 133–147
- Goodwin S. P., Whitworth A., 2007, *A&A*, 466, 943
- Grebel E. K., 2005, in Corbelli E., Palla F., Zinnecker H., eds, *ASSL Vol. 327: The Initial Mass Function 50 Years Later The IMF and mass segregation in young galactic starburst clusters*. pp 153–+
- Grether D., Lineweaver C. H., 2006, *ApJ*, 640, 1051
- Hillenbrand L. A., Bauermeister A., White R. J., 2008, in van Belle G., ed., *14th Cambridge Workshop on Cool Stars, Stellar Systems, and the Sun Vol. 384 of Astronomical Society of the Pacific Conference Series, An Assessment of HR Diagram Constraints on Ages and Age Spreads in Star-Forming Regions and Young Clusters*. pp 200–+
- Hurley J. R., 2003, in Makino J., Hut P., eds, *IAU Symposium Cluster CMDs from N-body Simulations: Stellar and Binary Evolution on GRAPE*. pp 113–+
- Hurley J. R., Pols O. R., Tout C. A., 2000, *MNRAS*, 315, 543
- Kiminki D. C., Kobulnicky H. A., Kinemuchi K., Irwin J. S., Fryer C. L., Berrington R. C., Uzpen B., Monson A. J., Pierce M. J., Woosley S. E., 2007, *ApJ*, 664, 1102
- Koen C., 2006, *MNRAS*, 365, 590
- Kouwenhoven M. B. N., Brown A. G. A., Goodwin S. P., Portegies Zwart S. F., Kaper L., 2008, *A&A*, submitted
- Kouwenhoven M. B. N., Brown A. G. A., Portegies Zwart S. F., Kaper L., 2007, *A&A*, 474, 77
- Kouwenhoven M. B. N., de Grijs R., 2008, *A&A*, 480, 103
- Kroupa P., 1995a, *ApJ*, 453, 350
- Kroupa P., 1995b, *MNRAS*, 277, 1491
- Kroupa P., 1995c, *MNRAS*, 277, 1507
- Kroupa P., 1995d, *ApJ*, 453, 358
- Kroupa P., 2001, *MNRAS*, 322, 231
- Kroupa P., 2002, *Science*, 295, 82
- Kroupa P., Bouvier J., 2003, *MNRAS*, 346, 343
- Kroupa P., Bouvier J., Duchêne G., Moraux E., 2003, *MNRAS*, 346, 354
- Kroupa P., Gilmore G., Tout C. A., 1991, *MNRAS*, 251, 293
- Kroupa P., Tout C. A., Gilmore G., 1993, *MNRAS*, 262, 545
- Kurucz R. L., 1992, in Barbuy B., Renzini A., eds, *IAU Symp. 149: The Stellar Populations of Galaxies Model Atmospheres for Population Synthesis*. pp 225–+
- Lucy L. B., 2006, *A&A*, 457, 629
- Maíz Apellániz J., 2008, *ApJ*, 677, 1278
- Maíz Apellániz J., Úbeda L., 2005, *ApJ*, 629, 873
- Malkov O., Zinnecker H., 2001, *MNRAS*, 321, 149
- Maschberger T., Kroupa P., 2008, submitted to *MNRAS*
- Mason B. D., Hartkopf W. I., Gies D. R., Henry T. J., Helsel J. W., 2008, *AJ*, in press (astro-ph/0811.0492)
- Massey P., 1998, in Gilmore G., Howell D., eds, *ASP Conf. Ser. 142: The Stellar Initial Mass Function (38th Herstmonceux Conference) The Initial Mass Function of Massive Stars in the Local Group*. pp 17–+

- Massey P., 2002, ApJS, 141, 81  
 Massey P., 2003, ARA&A, 41, 15  
 Massey P., Hunter D. A., 1998, ApJ, 493, 180  
 Metchev S., Hillenbrand L., 2008, ApJ, in press (astro-ph/0808.2982)  
 Meynet G., Maeder A., 2003, A&A, 404, 975  
 Oey M. S., Clarke C. J., 2005, ApJ, 620, L43  
 Parker J. W., Zaritsky D., Stecher T. P., Harris J., Massey P., 2001, AJ, 121, 891  
 Pfalzner S., Olczak C., 2007, A&A, 475, 875  
 Pflamm-Altenburg J., Kroupa P., 2006, MNRAS, 373, 295  
 Pflamm-Altenburg J., Kroupa P., 2007, MNRAS, 375, 855  
 Piskunov A. E., Belikov A. N., Kharchenko N. V., Sagar R., Subramaniam A., 2004, MNRAS, 349, 1449  
 Preibisch T., Zinnecker H., 1999, AJ, 117, 2381  
 Sagar R., Richtler T., 1991, A&A, 250, 324  
 Salpeter E. E., 1955, ApJ, 121, 161  
 Sana H., Gosset E., Nazé Y., Rauw G., Linder N., 2008, MNRAS, 386, 447  
 Schnurr O., Casoli J., Chené A.-N., Moffat A. F. J., St-Louis N., 2008, MNRAS, 389, L38  
 Sirianni M., Nota A., De Marchi G., Leitherer C., Clampin M., 2002, ApJ, 579, 275  
 Sirianni M., Nota A., Leitherer C., De Marchi G., Clampin M., 2000, ApJ, 533, 203  
 Stolte A., Brandner W., Brandl B., Zinnecker H., 2006, AJ, 132, 253  
 Thies I., Kroupa P., 2007, ApJ, 671, 767  
 Thies I., Kroupa P., 2008, MNRAS, 390, 1200  
 Tokovinin A., 2008, MNRAS, 389, 925  
 Turner N. H., ten Brummelaar T. A., Roberts L. C., Mason B. D., Hartkopf W. I., Gies D. R., 2008, AJ, 136, 554  
 Vanbeveren D., 1982, A&A, 115, 65  
 Vesperini E., McMillan S. L. W., Portegies Zwart S. F., 2006, Modelling Dense Stellar Systems, 26th meeting of the IAU, Joint Discussion 14, 22-23 August 2006, Prague, Czech Republic, JD14, #36, 14  
 Weidner C., Kroupa P., 2004, MNRAS, 348, 187  
 Weidner C., Kroupa P., 2006, MNRAS, 365, 1333  
 Weidner C., Kroupa P., Goodwin S. P., 2008, MNRAS, in preparation  
 Wyse R. F. G., Gilmore G., Houdashelt M. L., Feltzing S., Hebb L., Gallagher J. S., Smecker-Hane T. A., 2002, New Astronomy, 7, 395  
 Zhao J.-L., Chen L., Wen W., 2006, Chinese Journal of Astronomy and Astrophysics, 6, 435

## APPENDIX A: THE STELLAR INITIAL MASS FUNCTION

The following multi-component power-law IMF is used throughout the paper:

$$\xi(m) = k \begin{cases} k' \left(\frac{m}{m_H}\right)^{-\alpha_0} & , m_{\text{low}} \leq m < m_H, \\ \left(\frac{m}{m_H}\right)^{-\alpha_1} & , m_H \leq m < m_0, \\ \left(\frac{m_0}{m_H}\right)^{-\alpha_1} \left(\frac{m}{m_0}\right)^{-\alpha_2} & , m_0 \leq m < m_1, \\ \left(\frac{m_0}{m_H}\right)^{-\alpha_1} \left(\frac{m_1}{m_0}\right)^{-\alpha_2} \left(\frac{m}{m_1}\right)^{-\alpha_3} & , m_1 \leq m < m_{\text{max}}, \end{cases} \quad (\text{A1})$$

with exponents

$$\begin{aligned} \alpha_0 &= +0.30 & , & 0.01 \leq m/M_\odot < 0.08, \\ \alpha_1 &= +1.30 & , & 0.08 \leq m/M_\odot < 0.50, \\ \alpha_2 &= +2.35 & , & 0.50 \leq m/M_\odot < 1.00, \\ \alpha_3 &= +2.35 & , & 1.00 \leq m/M_\odot < m_{\text{max}} \end{aligned} \quad (\text{A2})$$

where  $dN = \xi(m) dm$  is the number of stars in the mass interval  $m$  to  $m + dm$ . The exponents  $\alpha_i$  represent the standard or canonical IMF (Kroupa 2001, 2002). The advantage of such a multi-part power-law description is the easy integrability and, more importantly, that *different parts of the IMF can be changed readily without affecting other parts*. Note that this form is a two-part power-law in the stellar regime, and that brown dwarfs contribute about 4 per cent by mass only and need to be treated as a separate population such that the IMF has a discontinuity near  $m_H = 0.08 M_\odot$  with  $k' \sim \frac{1}{3}$  (Kroupa et al. 2003; Thies & Kroupa 2007, 2008). A log-normal form below  $1 M_\odot$  with a power-law extension to high masses was suggested by Chabrier (2003) but is indistinguishable from the canonical form (Dabringhausen et al. 2008) and does not cater for the discontinuity. The observed IMF is today understood to be an invariant Salpeter/Massey power-law slope (Salpeter 1955; Massey 2003) above  $0.5 M_\odot$ , being independent of the cluster density and metallicity for metallicities  $Z \gtrsim 0.002$

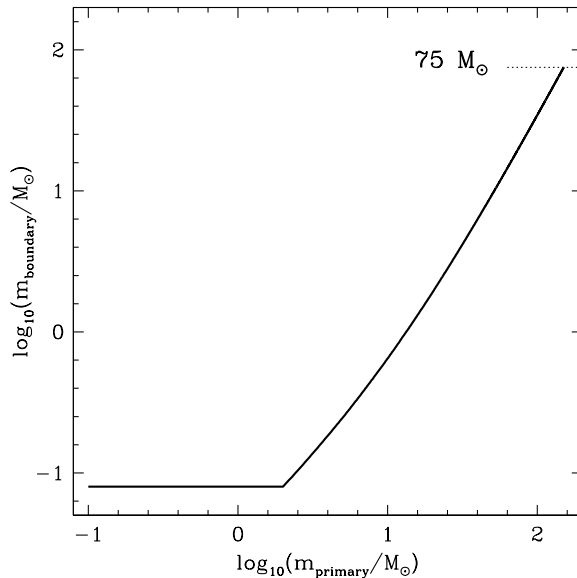


**Figure B1.** The minimum possible secondary mass ( $m_{\text{boundary}}$ ) in dependence of  $m_{\text{primary}}$ , both in logarithmic units (eq. B1). Indicated by a dotted line is the lower limit for the secondary mass for a primary of  $150 M_{\odot}$ .

(Massey & Hunter 1998; Sirianni et al. 2000, 2002; Parker et al. 2001; Massey 1998, 2002, 2003; Wyse et al. 2002; Bell et al. 2003; Piskunov et al. 2004; Pflamm-Altenburg & Kroupa 2006).

The basic assumption underlying our approach is the notion that all stars in every cluster are drawn from this same universal parent IMF, which is consistent with observational evidence (Elmegreen 1999; Kroupa 2001).

It should be noted here that, while not indicated in eq. A2, there is evidence of a maximal mass for stars ( $m_{\text{max}^*} \approx 150 M_{\odot}$ , Weidner & Kroupa 2004), a result confirmed by several independent studies (Oey & Clarke 2005; Figer 2005; Koen 2006), and that a maximal-star-mass–star-cluster-mass relation,  $m_{\text{max}}(M_{\text{ecl}}) \leq m_{\text{max}^*}$ , exists (Weidner & Kroupa 2006).

## APPENDIX B: SPECIAL TREATMENTS TO PRODUCE SECONDARY STARS

### B1 Special Pairing (SpP)

The following description has been developed in order to produce multiple stars for which the mass-ratio increases with increasing primary mass. Brown dwarfs ( $m < 0.08 M_{\odot}$ ) are not included as they are most likely to be treated as a separate population (Thies & Kroupa 2007, 2008).

In the regime above  $2 M_{\odot}$  the following quadratic relation was chosen to define the range of mass ratios as a fraction of the primary star mass,  $m_{\text{primary}}$ : the least massive allowed companion,  $m_{\text{boundary}}$ ,

$$m_{\text{boundary}} = 3.1 \cdot 10^{-3} \times m_{\text{primary}}^2 + 0.034 \times m_{\text{primary}}. \quad (\text{B1})$$

Companions are paired randomly within the so defined mass range. This eq. assures that primaries of up to  $2 M_{\odot}$  have a least-massive companion of  $0.08 M_{\odot}$ , while the least-massive companion is  $75 M_{\odot}$  for the most massive stars considered here ( $150 M_{\odot}$ ). Fig. B1 shows the minimum possible secondary mass ( $m_{\text{boundary}}$ ) in dependence of  $m_{\text{primary}}$  resulting from eq. B1.

Stellar masses are created by randomly drawing all stars from the IMF. Binaries are then made from this set of stars as described in § 2.1.

The combined range of possible  $q$ -values for eq. B1 and random pairing for stars below  $2 M_{\odot}$  is shown in Fig. B2. The solid line marks the minimum allowed mass ratio. The companion masses lie within the shaded region.

Fig. B3 shows the resulting  $q$ -distribution for 4 different mass bins. While the lowest mass bin ( $0.08 - 2 M_{\odot}$ ) shows a flat distribution resulting from random pairing the other three bins are peaked towards the lower edge of allowed mass-ratios. This is due to the steep power-law slope of the canonical IMF, which makes it highly likely that the chosen companion for a massive star is close to the lower limit  $m_{\text{boundary}}$ .

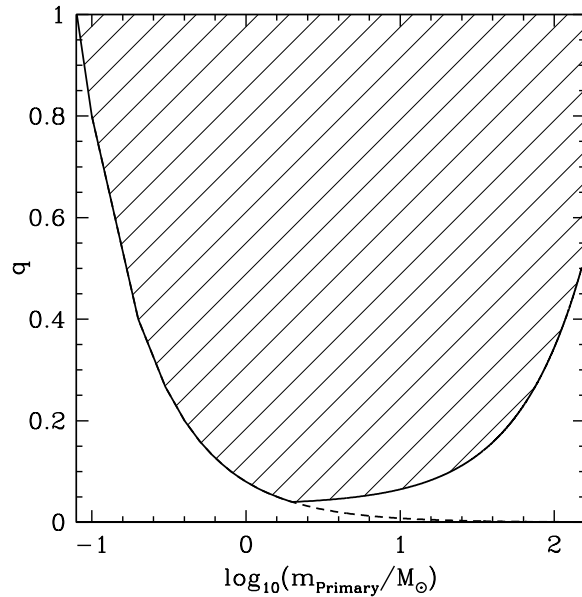


**Figure B2.** The possible  $q$ -values (*shaded region*) in dependence of the primary mass (in logarithmic units) produced by the SpP procedure (Appendix B1). Inside the *shaded region* the companions are randomly drawn from the IMF. The *dashed line* shows the minimum possible  $q$ -value for random sampling over all masses with a companion minimum mass of  $0.08 M_{\odot}$ .

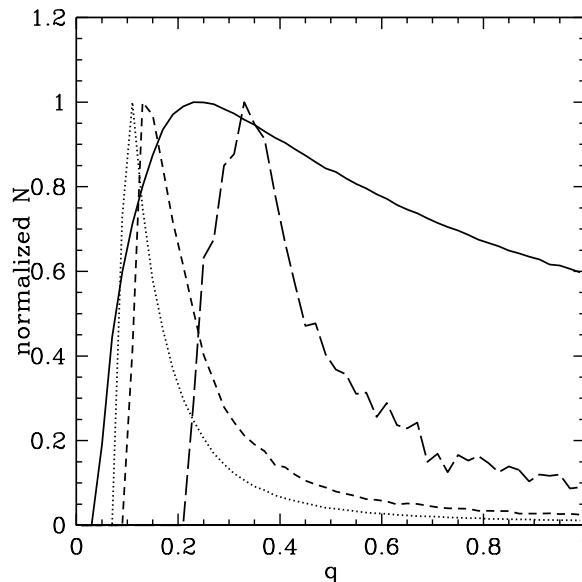


**Figure B3.** The mass-ratio ( $q$ ) distributions for primaries in several mass intervals for the SpP model. *Solid line:*  $m_{\text{primary}}$  from  $0.08$  to  $2 M_{\odot}$ , *dotted line:*  $2 - 10 M_{\odot}$ , *short-dashed line:*  $10 - 50 M_{\odot}$  and *long-dashed line:*  $50 - 100 M_{\odot}$ .

## B2 System Pairing (SyP)

In order to obtain systems with components which are strongly biased towards equal mass systems, the SyP scheme is motivated by the possible merger origin of massive stars and may also be applicable for the competitive accretion scenario. System masses are drawn randomly from the adopted fixed system IMF and then split into companions as follows:

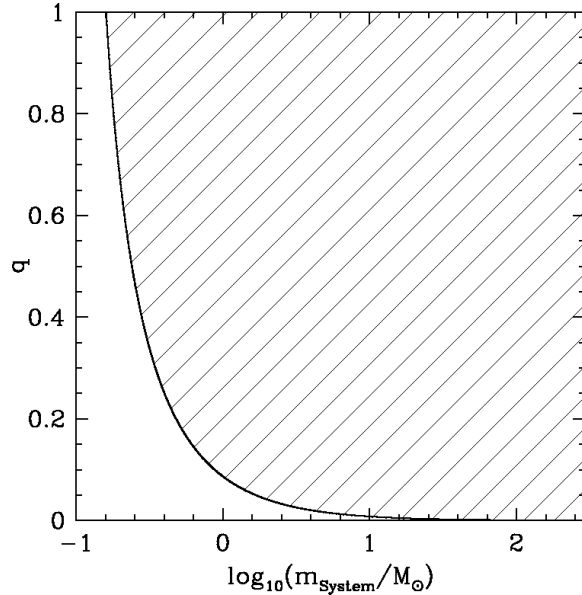


**Figure B4.** The possible  $q$ -values (*shaded region*) in dependence of the system mass (in logarithmic units) produced by the SyP procedure (Appendix B2). But within the *shaded region* the  $q$ -values are only randomly distributed for  $m_{\text{system}} < 10M_{\odot}$ . Above this mass the  $q$ -values are from distributions as shown in Fig. B6.

For  $m_{\text{system}} > 10M_{\odot}$ :

$$q = \frac{m_{\text{system}} \times R}{10}; \quad (\text{B2})$$

$$\text{if } q > 0.9 : q = (0.1 \times R) + 0.9; \quad (\text{B3})$$

$$m_{\text{primary}} = \frac{m_{\text{system}}}{1 + q}; \quad (\text{B4})$$

$$m_{\text{companion}} = m_{\text{system}} - m_{\text{primary}}, \quad (\text{B5})$$

where  $R$  is a random number between 0 and 1. This formulation biases the mass ratio distribution for massive stars strongly towards more massive companions while still allowing for occasional low-mass secondaries. Systems less-massive than  $10 M_{\odot}$  are split randomly in two or more halves with the limitation that the lower limit for the stellar mass of the companions is  $0.08 M_{\odot}$ .

The IMF for the systems is the same as in § A but with different mass intervals. The lowest *system mass* allowed is  $0.16 M_{\odot}$  and the highest  $300 M_{\odot}$  and the exponent changes at  $1 M_{\odot}$  instead of  $0.5 M_{\odot}$ . But for the *stars* produced from these systems the lower and upper mass limits are still  $0.08$  and  $150 M_{\odot}$ .

The combined range of possible  $q$ -values is shown in Fig. B4 while the probabilities for the companion masses for a few examples are shown in Fig. B5. These probabilities are chosen randomly from a Gaussian distribution between  $m_{\text{boundary}}$  and the maximum possible mass for the secondary,  $m_{\text{sec,max}}$ , which is  $\frac{m_{\text{system}}}{2}$ . The mean of the Gaussian is  $m_{\text{sec,max}}$  and its dispersion is given by  $\sigma = m_{\text{sec,max}} / (0.064m_{\text{system}} + 3.29)$ .

In Fig. B6 the  $q$ -distribution is shown for 4 different mass bins. The three bins with stars above  $10 M_{\odot}$  peak strongly above  $q = 0.8$ , indicating the strong tendency to produce nearly equal mass binaries with this algorithm.

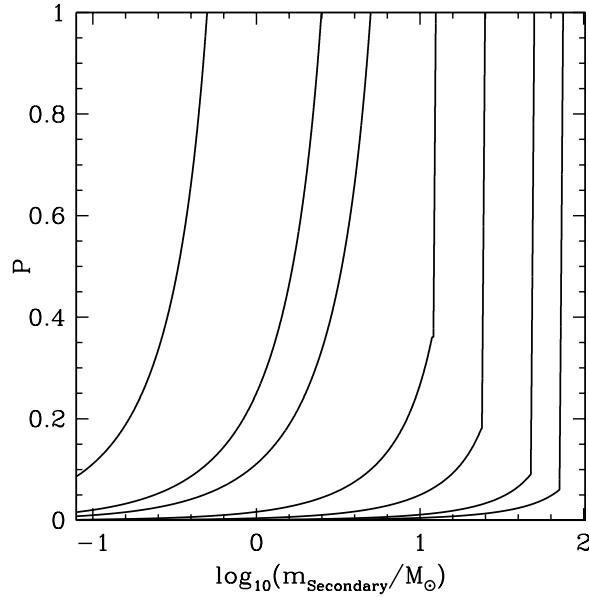


**Figure B5.** The probability  $P$  to pick the companion mass between the lower limit ( $0.08 M_{\odot}$ ) and half of the system mass for system masses of (from left to right ) 1, 5, 10, 25, 50, 100 and  $150 M_{\odot}$ .

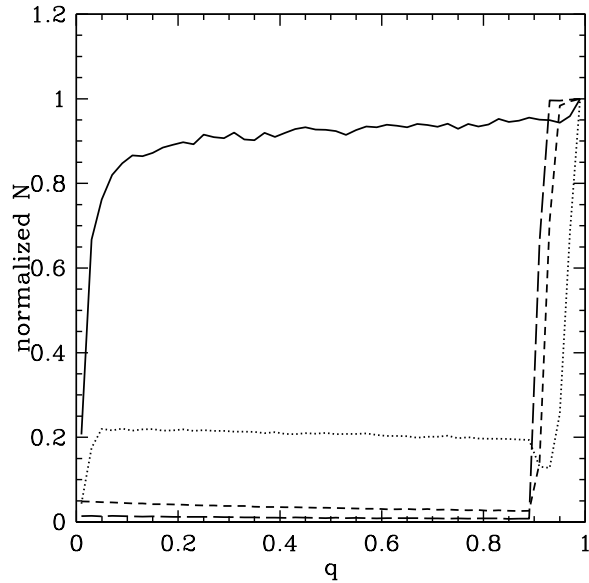


**Figure B6.** The mass-ratio ( $q$ ) distributions for primaries in several mass intervals (Appendix B2). *Solid line:*  $m_{\text{primary}}$  from  $0.08$  to  $2 M_{\odot}$ , *dotted line:*  $2 - 10 M_{\odot}$ , *short-dashed line:*  $10 - 50 M_{\odot}$  and *long-dashed line:*  $50 - 100 M_{\odot}$ . The mass-ratio distribution for low-mass stars (*solid line*) is not completely flat due to the lower mass limit for stars of  $0.08 M_{\odot}$ .

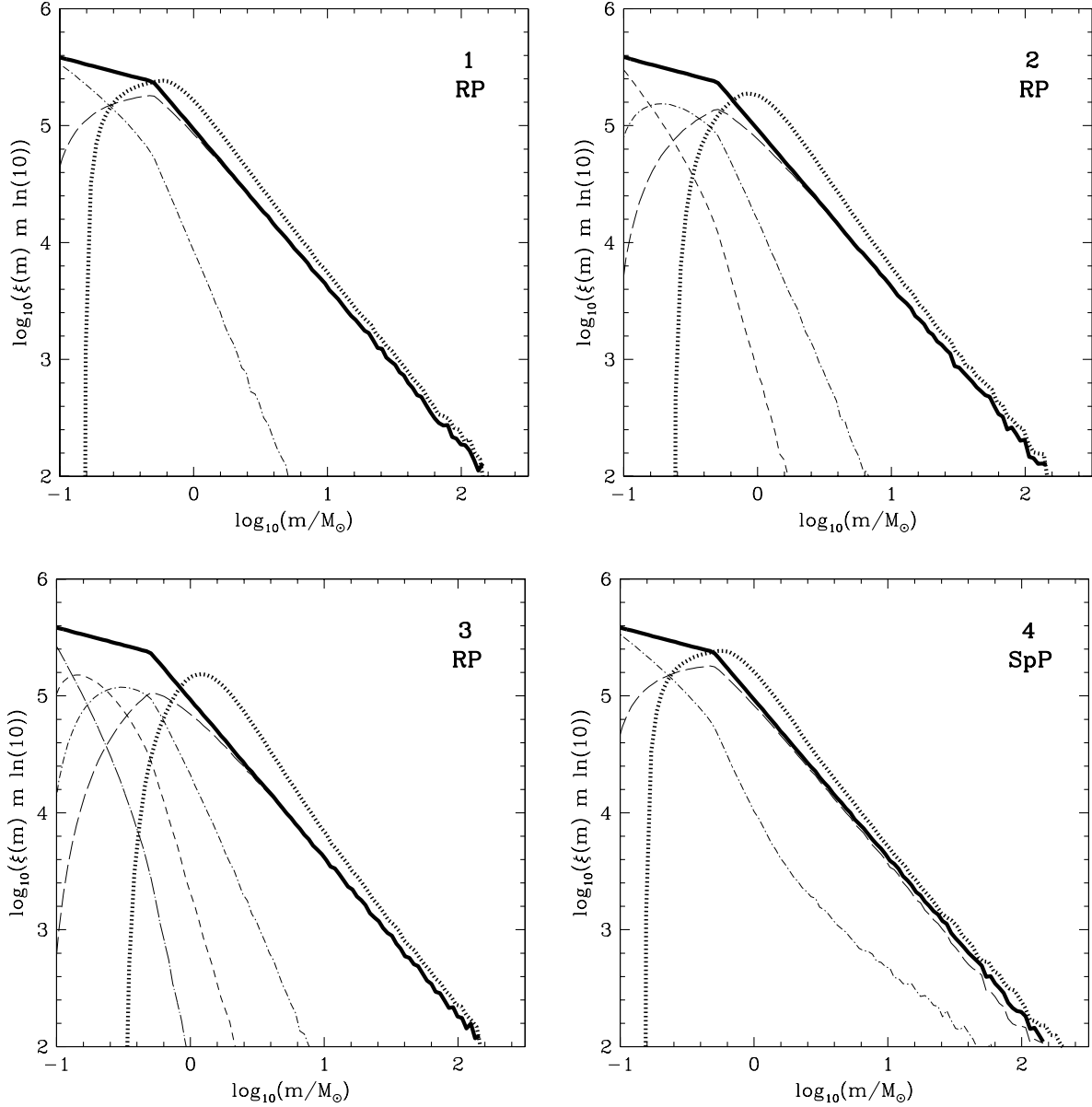


**Figure C1.** IMFs of Models 1 to 4. The *thick solid lines* are the IMFs of all stars, the *thin solid lines* are the input IMFs (identical to the IMF of all stars for models 1 to 6), the *thick dotted lines* the system IMFs and the *thin lines* represent the mass functions for the individual components. The *thin long-dashed lines* are the primary star IMFs, the *thin dash-dotted lines* are the secondary star IMFs, the *thin short-dashed lines* are the tertiary star IMFs (only panels 2, 3, 5, 6, 8 and 9) and the *thin long-dash-dotted lines* are the quaternary star IMFs (only panels 3, 6 and 9). The “spikes” in the system IMFs (*thick dotted lines*) in panels 4 to 10 are a result of changing the  $q$ -distribution at  $2 M_{\odot}$ .

## APPENDIX C: IMFS WITHOUT STELLAR EVOLUTION

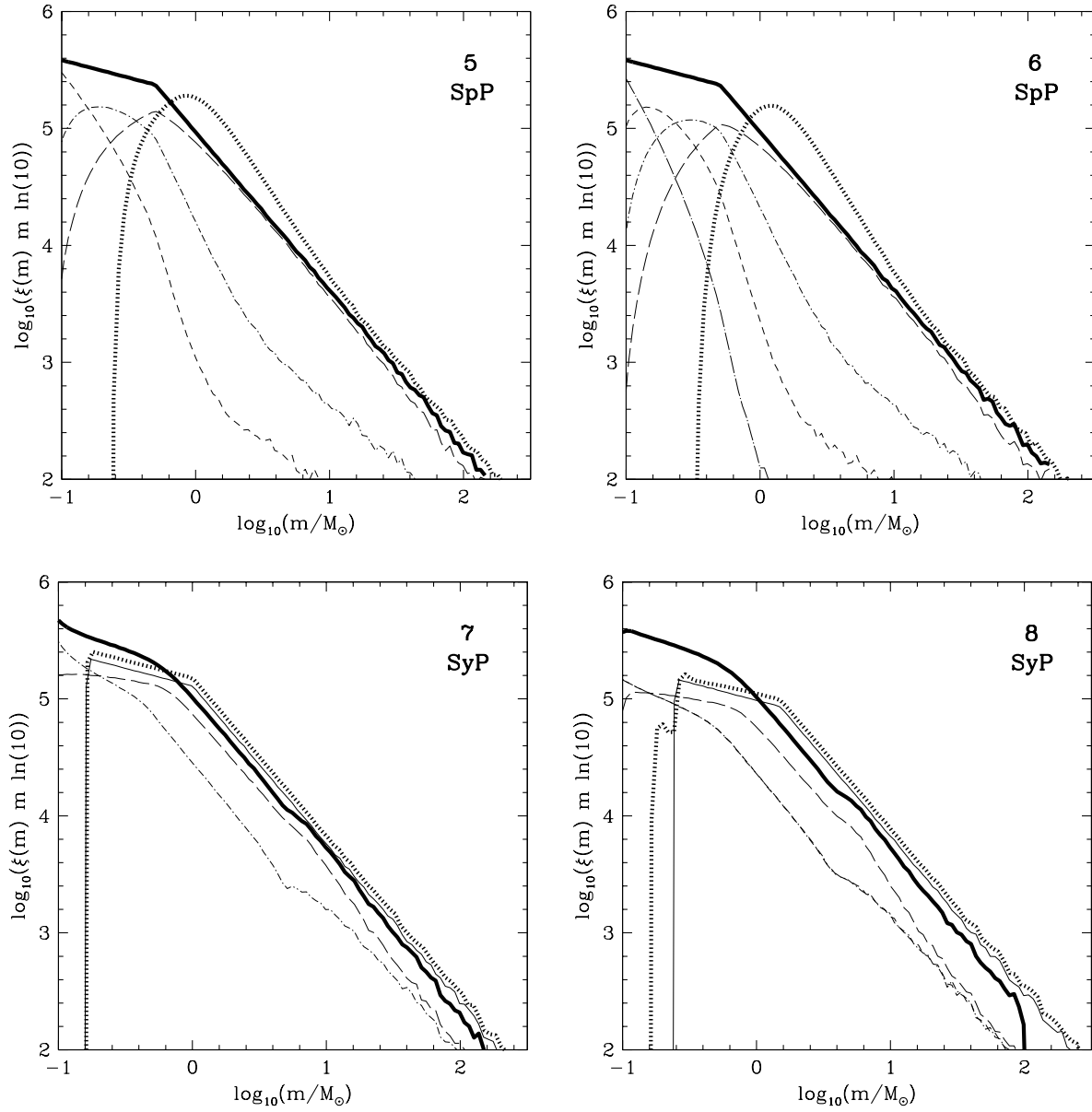


**Figure C2.** Like Fig. C1 but for the Models 5 to 8 from Table 2.

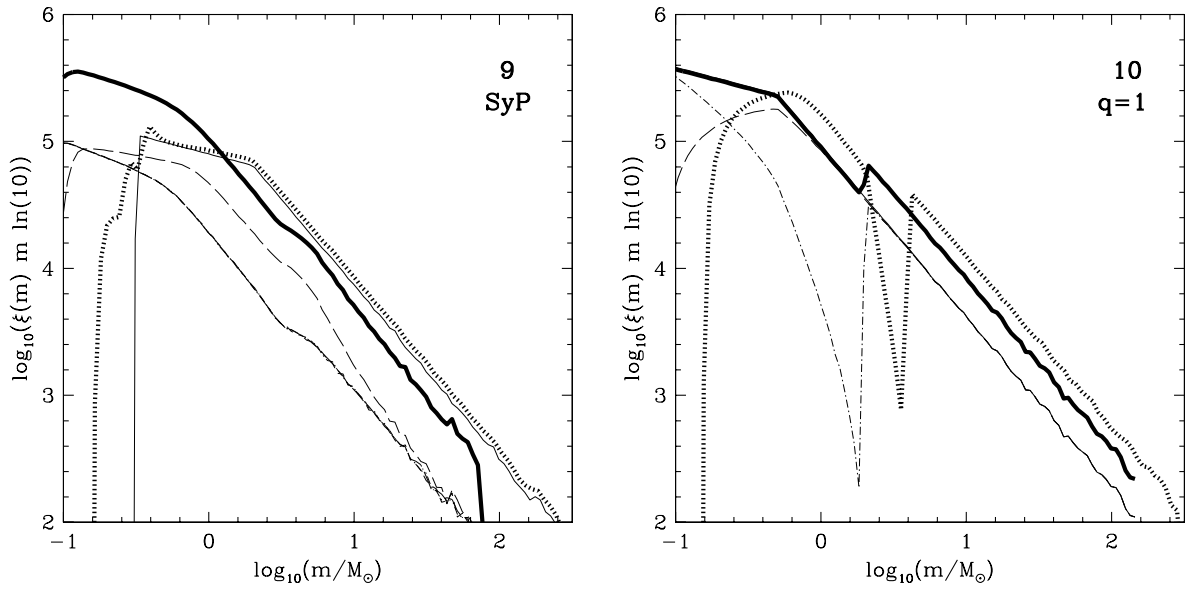
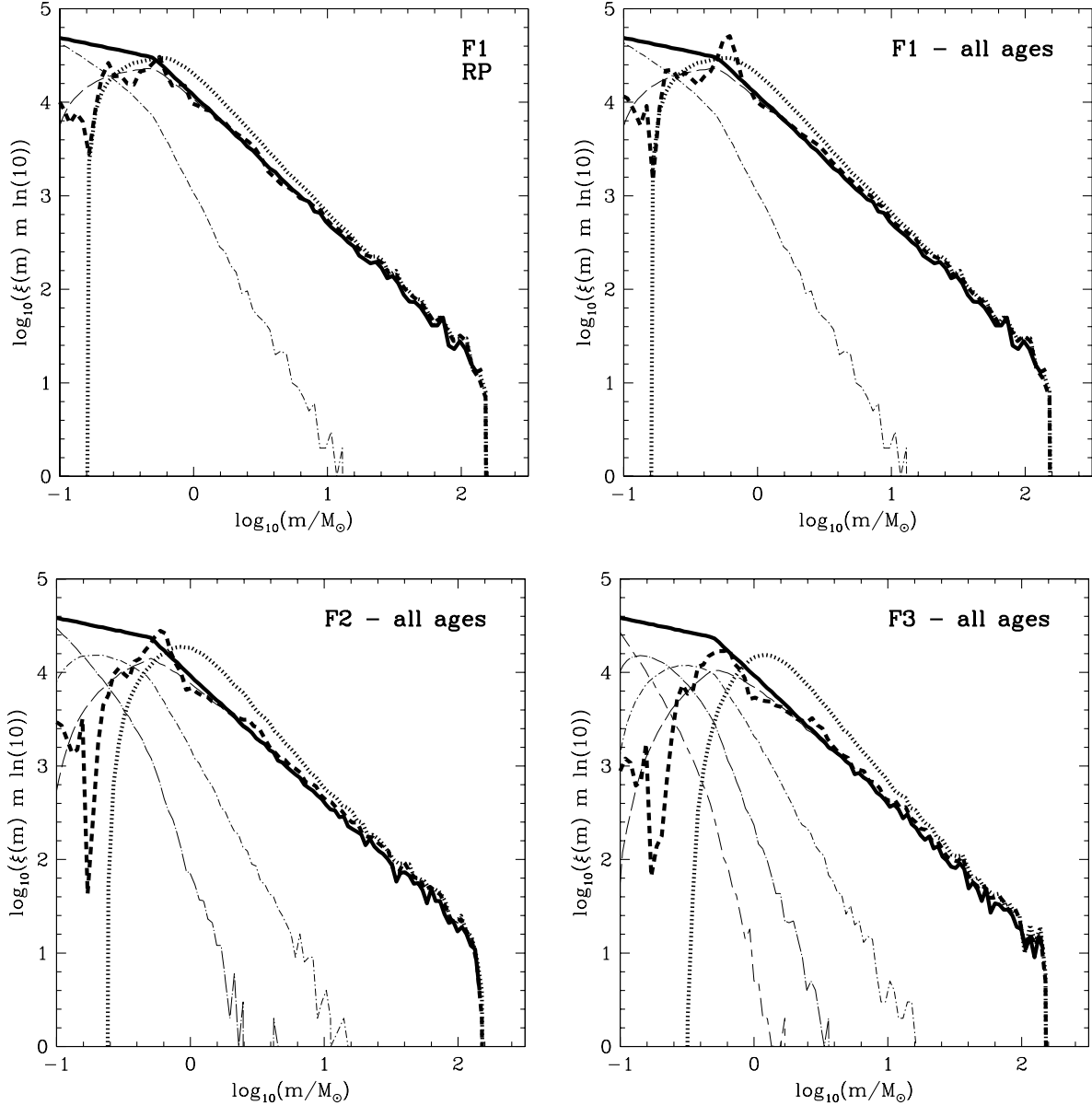
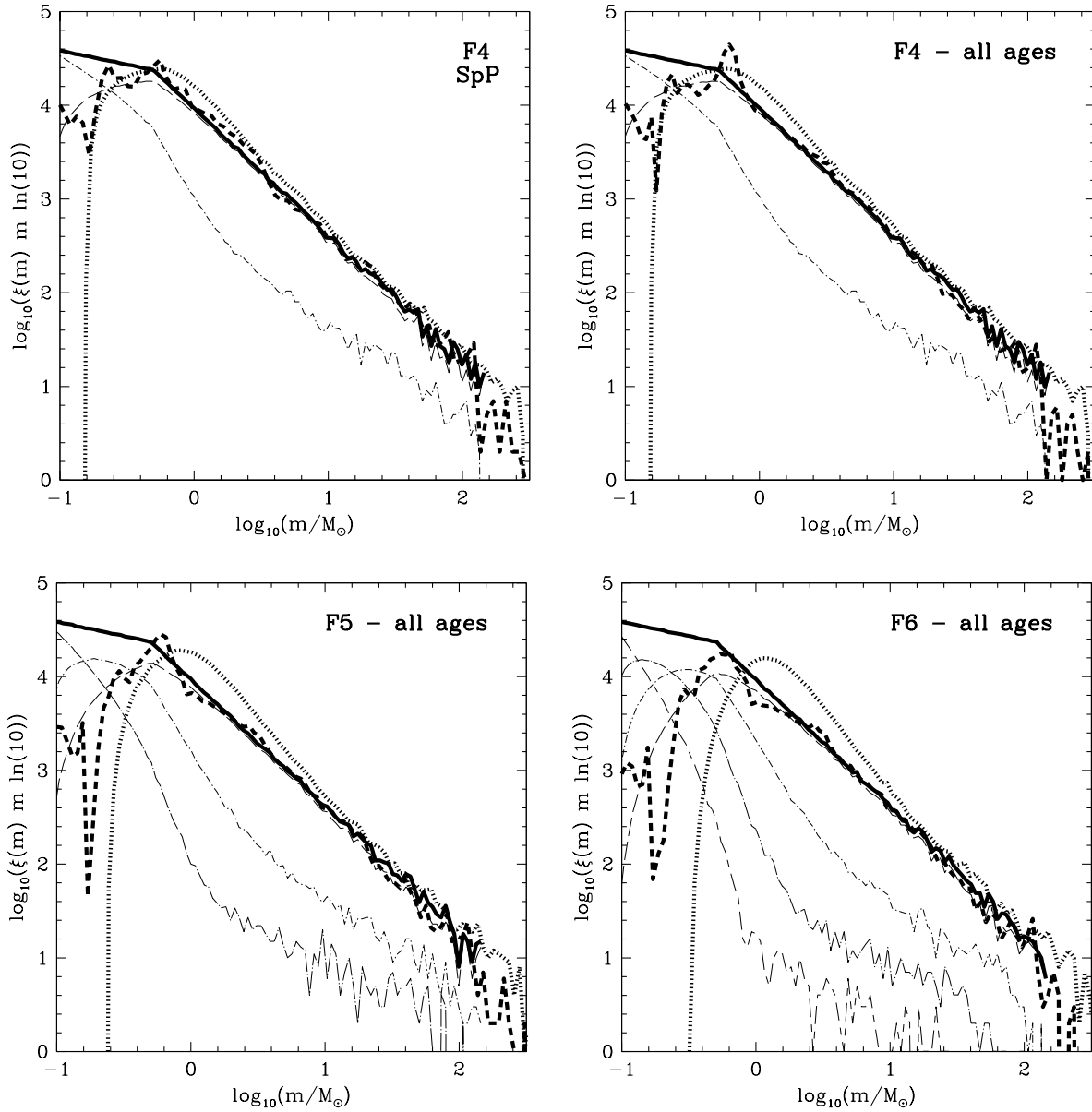


Figure C3. Like Fig. C1 but for the Models 9 and 10 from Table 2.



**Figure D1.** IMFs of Models Fit 1 to Fit 3 from Table 3. *Thick solid lines* are the input IMFs, the *thick dotted lines* are the system IMFs without stellar evolution, the *thick short-dashed lines* are the “observed” IMFs, the *long-dashed lines* are the primary star IMFs, the *dash-dotted lines* are the secondary star IMFs, the *thin short-dashed lines* are the tertiary star IMFs (only Models Fit 2, 3, 5, 6, 8 and 9) and the *thin long-dash-dotted lines* are the quarternary star IMFs (only Models Fit 3, 6 and 9). For the first panel (“F1 RP”) the “observed” IMF is created only from recovered stars with pseudo ages less than 5 Myr. For each of the other three panels all recovered stars regardless of their ages are used. These panels are marked by “all ages”. Note the dip in all models around  $\log_{10}(m) \approx -0.8$  (about  $0.16 M_{\odot}$ ). It is the result of differences in the PMS tracks from different authors used here. These differences shift some of the stars between 0.15 and  $0.3 M_{\odot}$  to lower masses but have no influence on the results of this study as we restrain ourselves only to the high-mass end of the IMF.

**APPENDIX D: IMFS WITH STELLAR EVOLUTION**



**Figure D2.** Like Fig. D1 but for the Models Fit 4 to Fit 6 from Table 3.

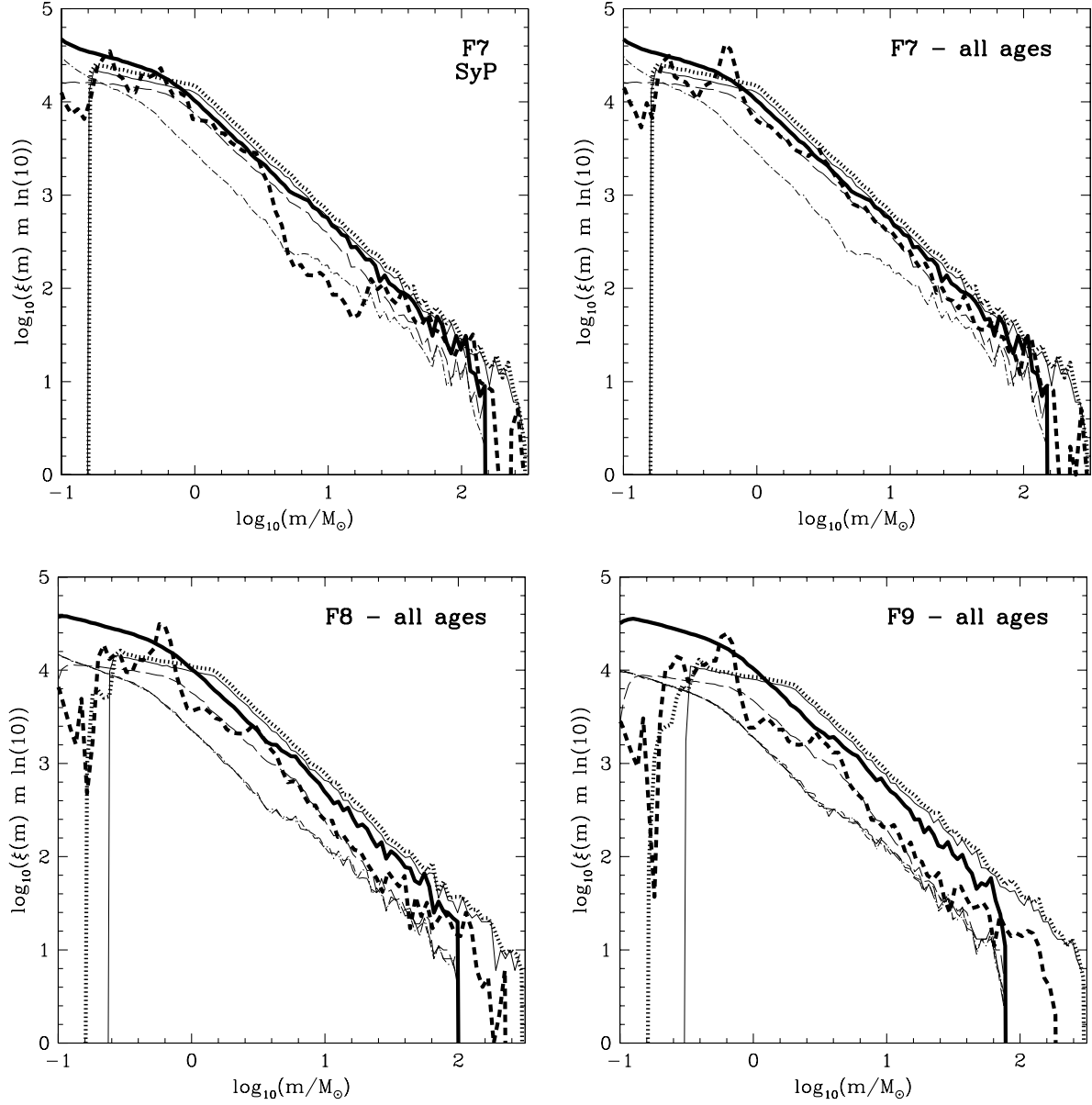


**Figure D3.** Like Fig. D1 but for the Models Fit 7 to Fit 9 from Table 3.

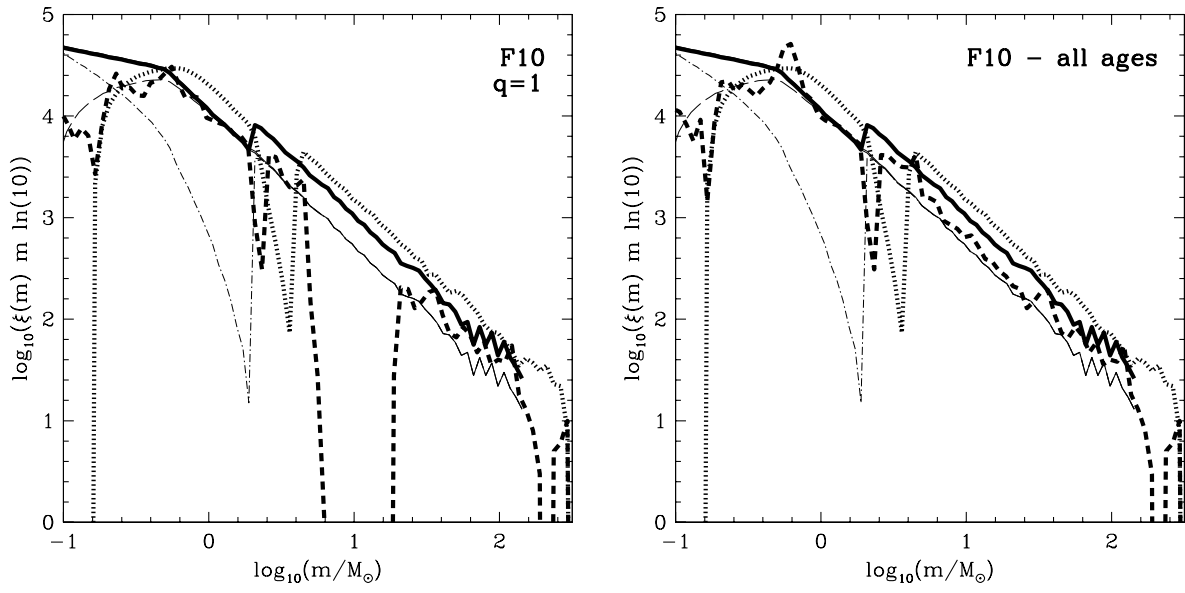


**Figure D4.** Like Fig. D1 but for the Model Fit 10 from Table 3.